


Cite this: *RSC Adv.*, 2023, **13**, 11096

Received 1st March 2023  
Accepted 31st March 2023

DOI: 10.1039/d3ra01383a

rsc.li/rsc-advances

# Anticancer therapeutic potential of benzofuran scaffolds

Ashraf A. Abbas  and Kamal M. Dawood \*

Benzofuran moiety is the main component of many biologically active natural and synthetic heterocycles. These heterocycles have unique therapeutic potentials and are involved in various clinical drugs. The reported results confirmed the extraordinary inhibitory potency of such benzofurans against a panel of human cancer cell lines compared with a wide array of reference anticancer drugs. Several publications about the anticancer potencies of benzofuran-based heterocycles were encountered. The recent developments of anticancer activities of both natural and synthetic benzofuran scaffolds during 2019–2022 are thoroughly covered. Many of the described benzofurans are promising candidates for development as anticancer agents based on their

Department of Chemistry, Faculty of Science, Cairo University, Giza, 12613, Egypt.  
E-mail: kmdawood@sci.cu.edu.eg; Fax: +20-2-35727556; Tel: +20-2-35676602



*Professor Ashraf A. Abbas was born in Egypt in September 1968 and he is presently Professor of Organic Chemistry, Department of Chemistry, Faculty of Science, Cairo University, Giza, Egypt since 2009. He graduated from Cairo University in 1990. He received his MSc and PhD degrees in 1994 and 1997, respectively, from Cairo University. He spent Six months in the Fakultät für Chemie, universität*

*of Konstanz (Germany) on a DAAD fellowship (1996) to finish his PhD thesis and one year in Tokyo Institute of technology (TIT, Japan) as UNESCO fellow (postdoctoral fellowship) from Oct 2001 to Sept 2002. He received several research prizes in chemistry; (1) he was awarded the prize of Prof. Dr Mohamed Abdel Salam in chemistry (2001) for young scientists provided by Academy of Scientific Research and Technology (Egypt). (2) He was awarded the Cairo university encouragement prize in Chemistry in 2004. (3) He was awarded the Third World Academy of Science (TWAS) prize in chemistry for young scientists in 2004 provided by ICTP-Strada, Trieste-Italy, (4) he was awarded the State Award in Chemistry, Egypt 2005. He published many papers in the field of synthesis and applications of macrocycles and bis-heterocycles chemistry.*



*Kamal M. Dawood graduated from Cairo University, Egypt in 1987 then carried out his MSc and PhD studies under the supervision of Professor Ahmad Farag, Cairo University and received his PhD in 1995. In 1997 he was awarded the UNESCO Fellowship at TIT for one year and in 1999 he was awarded the JSPS Fellowship for two years and in both fellowships he worked with Professor*

*T. Fuchigami at Tokyo Institute of Technology (TIT) in the field of "Anodic Selective Fluorination of Heterocycles". Further, he was awarded the Alexander von Humboldt (AvH) Fellowship at Hannover University in 2004–2005 with Prof. A. Kirschning (in the area of polymer supported palladium catalyzed cross coupling reactions) and as AvH three short visits in 2007, 2008 and 2012 with Prof. P. Metz at TU-Dresden (in the field of Metathesis Reactions in Domino Processes). Since May 2007 – to date, he has been appointed as full Professor of Organic Chemistry, Faculty of Science, Cairo University. He worked as Professor of Organic Chemistry at Chemistry Department, Kuwait University from Sept. 2013 till Aug 2017. He received a number of National Awards: Cairo University Award in Chemistry (2002), the State-Award in Chemistry (2007), Cairo University Award for Academic Excellence (2012) and Cairo University Merit Award (2017). He published about 150 scientific papers and reviews in distinguished international journals. There are more than 3300 citations of his work (Scopus h-index 30).*



outstanding inhibitory potency against a panel of human cancer cells compared with reference anticancer drugs. These findings encourage medicinal chemists to explore new areas to improve human health and reduce suffering.

## 1. Introduction

Heterocyclic fragments widely exist in a broad array of natural products. Many such versatile natural products have unique pharmacological properties and constitute the main core of several drugs in the market.<sup>1,2</sup> In particular, the benzofuran moiety is commonly available in a large number of promising natural products and natural drugs.<sup>3,4</sup> Thus, great interest has been focused on the synthesis and extraction of benzofuran-based heterocycles due to their pronounced importance in pharmaceutical and agricultural fields.<sup>5,6</sup> Natural benzofurans are characterized by their distinctive wide range of biological properties. For example, the naturally occurring benzofuranones (**Aurones**) (Fig. 1) showed promising anticancer properties.<sup>7–10</sup> **Salvianolic acid B** and **Ganodone** are two examples of naturally occurring benzofuran derivatives that are used as potential natural sources of anticancer medicines (Fig. 1).<sup>11–14</sup> The natural **isobenzofuran** derivative is found in edible mushroom.<sup>15,16</sup> Interestingly, some natural and synthetic approved drugs contain a benzofuran unit, such as **Griseofulvin** (Antibiotics drug), **Dronedarone** and **Amiodarone** (Antiarrhythmic drugs), **Ramelteon** (Sedative drug), **Vilazodone** and **Citalopram** (Anti-depressive drugs), **Saprisartan** (anti-hypertension drug) and **Benzbromarone** (for gut treatment) are depicted in Fig. 2. **Moracin** (hydroxylated 2-arylbenzofuran derivatives) is another class of highly bioactive natural products that contains a benzofuran moiety (Fig. 1).<sup>17,18</sup> Such benzofuran members are lead structures in drug development and some of them have

promising anticancer activities.<sup>19,20</sup> In addition, among the natural products that contain benzofuran moiety is rocaglamide and its analogues, which are of great interest as highly potent anticancer agents.<sup>21,22</sup> Moreover, many synthetic benzofuran compounds are reported to have significant anticancer activities.<sup>23,24</sup>

Recently, our research interest was focused on the biological applications of benzofuran derivatives and other heterocycles of potent anticancer activities.<sup>25–29</sup> Herein, we report an updated comprehensive outlines of the recent developments (2019–2022) of the anticancer potentiality of both natural and synthetic bioactive benzofuran-based compounds as a highly significant source for drug development and discovery.

## 2. Anticancer activity of benzofuran derivatives

### 2.1. Anticancer activity of benzofuran-3-carboxaldehyde derivatives

Chen *et al.* reported the two benzofuran derivatives **1** and **2**, naturally isolated from mangrove endophytic fungus *Fusarium* sp. 2ST2, and tested their cytotoxicity against five human cancer cell lines; A549 (lung), HeLa (cervical), KYSE150 (esophageal squamous), PC-3 (pancreatic), and MDA-MB-435 (breast) cancers. Unfortunately, the reported compounds showed non-promising activity against all of the studied cancer cell lines at 50  $\mu$ M concentration.<sup>30</sup>

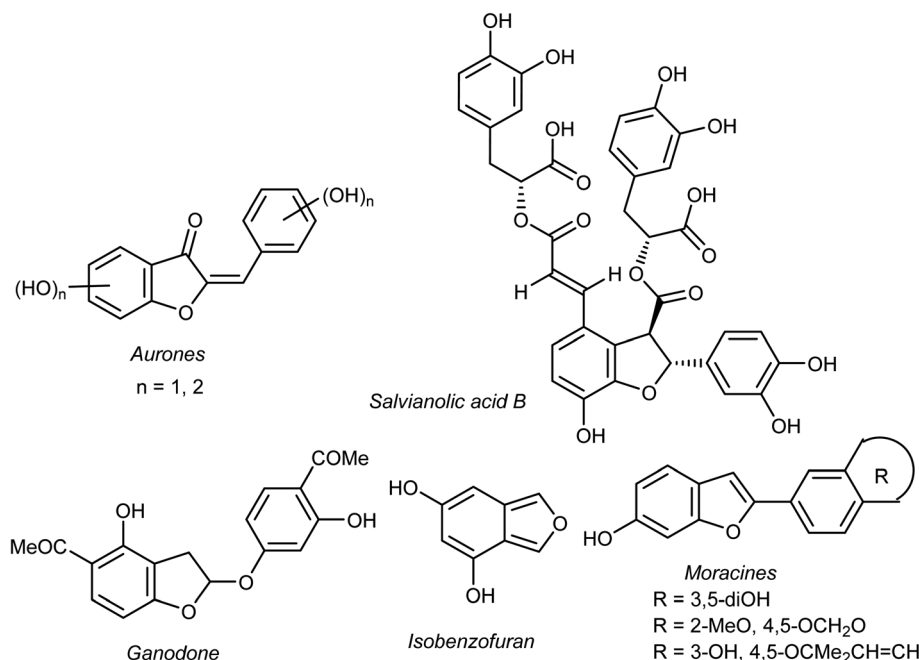


Fig. 1 Structures of some natural benzofuran derivatives with anticancer activities.

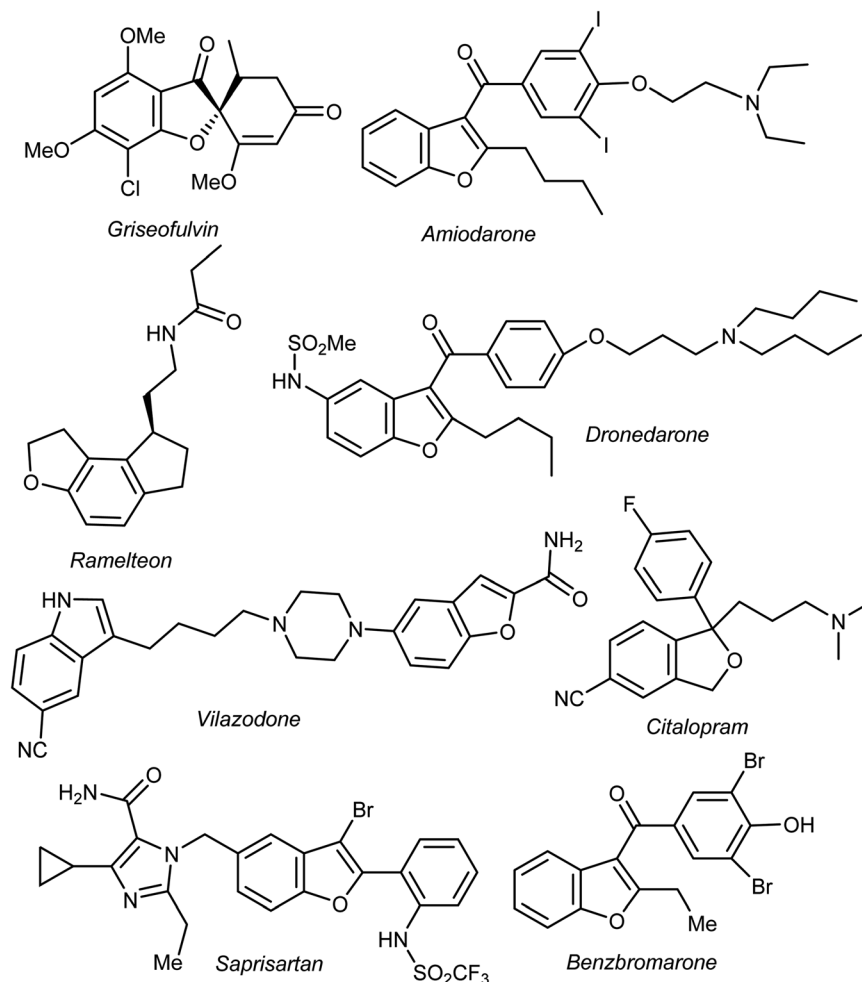
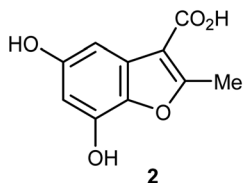
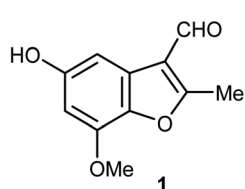
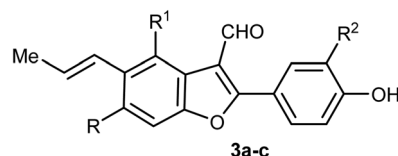


Fig. 2 Some clinical drugs containing benzofuran scaffolds.



Structures of benzofuran derivatives 1 and 2

Lang *et al.* isolated five derivatives of 3-formylbenzofuran **3a-d** from the 95% EtOH extract of *Itea yunnanensis*, and screened their anti-hepatocellular carcinoma (HCC) activity by MTT assay [MTT is 3-[4,5-dimethylthiazol-2-yl]-2,5 diphenyltetrazolium bromide]. The derivatives **3b** and **3c** displayed promising growth inhibition potency on SK-Hep-1 cells (with  $IC_{50}$  = 5.365 and 6.013  $\mu$ M, respectively) compared with the standard control sorafenib ( $IC_{50}$  = 9.452  $\mu$ M). The mechanistic study proved that compound **3b** significantly reduced the phosphorylation level of ERK (extracellular signal-related kinase), which suggested that **3b** stopped cell growth and promoted apoptosis of SK-Hep-1 cells by blocking RAS/RAF/MEK/ERK signaling pathway. Thus, the 3-formylbenzofuran derivatives **3b** and **3c** had the potential to be lead structures as anti-hepatocellular carcinoma agents.<sup>31</sup>



- 3a: R=R<sup>1</sup>= H; R<sup>2</sup>= OH  
 3b: R=R<sup>1</sup>=R<sup>2</sup>= OH  
 3c: R=H. R<sup>1</sup>=R<sup>2</sup>= OH  
 3d: R=R<sup>1</sup>=R<sup>2</sup>= H

Structure of 3-formylbenzofuran derivatives 3a-d

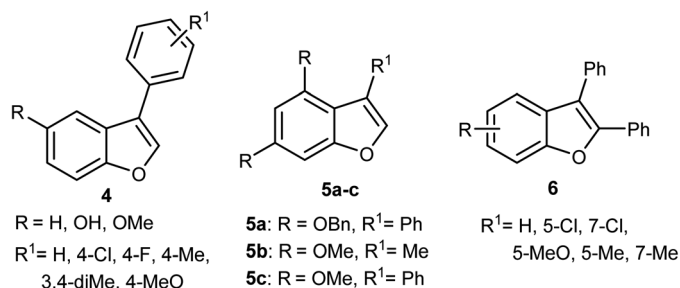
## 2.2. Anticancer activity of 2(3)-phenylbenzofuran derivatives

Some benzofuran scaffolds **4-6** were found to be good inhibitors of Pin1 (peptidyl-prolyl *cis-trans* isomerase NIMA-interacting 1); Pin1 had an oncogenic role in multiple human cancers particularly hepatocellular carcinoma (HCC). Particularly, 4,6-di(benzyloxy)-3-phenylbenzofuran **5a** revealed an excellent selectivity towards Pin1 (with  $IC_{50}$  = 0.874  $\mu$ M) with 75.38% inhibition. This was a stronger activity compared to juglone. A cell-based biological study proved that **5a** appreciably suppressed cell proliferation of HCC cells *via* restoring the

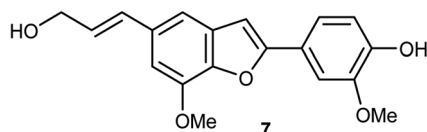


## Review

nucleus-to-cytoplasm export of XPO5 and upregulating mature miRNAs expression. The Pin1 inhibitor **5a** increased the biogenesis of tumor suppressor miRNAs (miR-122 and miR-29b) and reduced the HCC cell proliferation. Thus, **5a** was considered as a promising guide structure for Pin1 inhibition with the therapeutic potential of miRNA-based treatment for human cancers.<sup>32</sup>

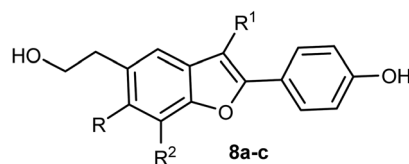
Structures of benzofuran scaffolds **4-6**

The anticancer activity of the naturally isolated benzofuran derivative (ailanthoidol) **7** (isolated from the barks of *Zanthoxylum ailanthoides*) was discussed by Tseng *et al.* Compound **7** displayed more potent cytotoxicity in Huh7 (mutant p53) hepatoma cells than in liver carcinoma (HepG2) cells (wild-type p53). The benzofuran derivative **7** decreased the cell viability in Huh7 cells, with IC<sub>50</sub> of 45 μM and 22 μM at 24 h and 48 h, respectively, while for HepG2 it had IC<sub>50</sub> > 80 μM. This compound induced G1 arrest and reduced the expression of cyclin D1 and CDK2 (Cyclin Dependent Kinase 2). This compound induced significant apoptosis in Huh7 cells as examined by flow cytometry analysis with annexin-V/PI staining. Compound **7** also increased the expression of cleaved PARP (poly-ADP ribose polymerase) and Bax (Bcl-2-associated X protein) and decreased the expression of procaspase 3/8 and Bcl-xL/Bcl-2. Thus, the mechanism of action revealed that compound **7** exhibited a more potent antiproliferation potential on mutp53 HCC than on wtp53 HCC cells due to the down-regulation of mutp53 and inactivation of the STAT3.<sup>33</sup>

Structure of the natural Ailanthoidol **7**

The biological activities of the natural compound **8a** and its synthetic derivatives **8b** and **8c** against five human cancer cell lines; HepG2, MCF-7, A549, PC3 (prostate carcinoma), and Hep3B (hepatocellular carcinoma) and various protein levels were reported. The experiments were conducted at 6 μM which was close to the IC<sub>50</sub> values of the tested compounds. The derivatives **8a-c** induced apoptotic cell death related PARP cleavage in HepG2, A549, MCF74, PC3, and Hep3B cancer cell

lines. In addition, the tumor inhibitor protein p53 was also induced in p53 wild-type cancer cells.<sup>34</sup>



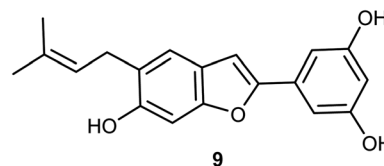
**8a**: R = H, R<sup>1</sup> = Me, R<sup>2</sup> = MeO

**8b**: R = MeO, R<sup>1</sup> = R<sup>2</sup> = H

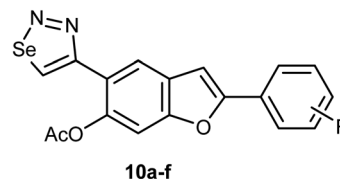
**8c**: R = R<sup>1</sup> = H, R<sup>2</sup> = MeO

Structure of the natural benzofuran derivatives **8a-c**

The naturally isolated benzofuran derivative **9**, isolated from the leaves of *Morus alba* L., was described as an inhibitor of cell proliferation that induced cell apoptosis in human non-small-cell lung carcinoma (NSCLC) cells, PC9 and A549 using MTT bioassay. Compound **9** treatment resulted in mitochondrial apoptosis in PC9 and A549 cells and also increased autophagy flux by the increase of autophagosome formation. Interestingly, the molecular mechanism of compound **9** against lung cancer through apoptosis and autophagy confirmed its importance as a therapeutic agent for NSCLC treatment. Compound **9** inhibited the growth of A549 and PC9 cells in a dose-dependent manner with IC<sub>50</sub> values of 48.4 μM and 6.6 μM, respectively. The great perspective of compound **9** as an anti-lung cancer agent, made it possible to be developed as a novel therapeutic agent for NSCLC treatment in the future.<sup>35</sup>

Structure of the natural benzofuran derivative **9**

Selenium-containing compounds exhibit a wide range of biological potencies including anticancer activity.<sup>36,37</sup> In particular, 1,2,3-selenadiazole-based benzofuran derivatives **10a-f** were prepared by Olomola *et al.* and screened for anti-proliferation activity against the breast cancer (MCF-7) and the human embryonic kidney derived (HEK-293-T) cell lines using the MTT assay. Most of the derivatives **10a-f** exhibited low to moderate inhibition except compound **10f** which showed promising antigrowth action against MCF-7 cells with IC<sub>50</sub> = 2.6



**10a**: R = H; **10b**: R = 3-F; **10c**: R = 4-F;

**10d**: R = 3-Cl; **10e**: R = 4-Me;

**10f**: R = 4-MeO

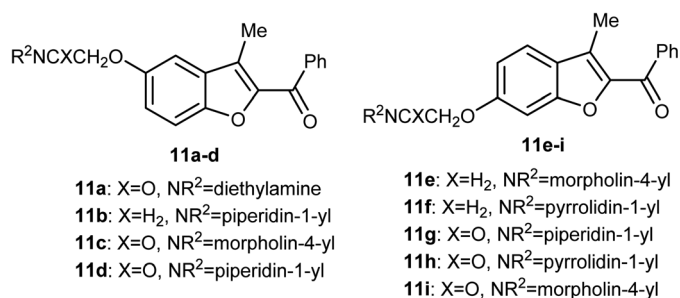
Structure of 1,2,3-selenadiazole-based benzofurans **10a-f**



$\mu\text{M}$  compared to doxorubicin ( $\text{IC}_{50} = 0.8 \mu\text{M}$ ). Compound **10f** was relatively less cytotoxic against the normal cell line ( $\text{IC}_{50} = 1.2 \mu\text{M}$ ). Compound **10a** exhibited, however, moderate effect against the MCF-7 cell line ( $\text{IC}_{50} = 7.1 \mu\text{M}$ ), but it was relatively more cytotoxic towards the Hek293-T cell line ( $\text{IC}_{50} = 3.5 \mu\text{M}$ ) compared to doxorubicin ( $\text{IC}_{50} = 1.2 \mu\text{M}$ ).<sup>38</sup>

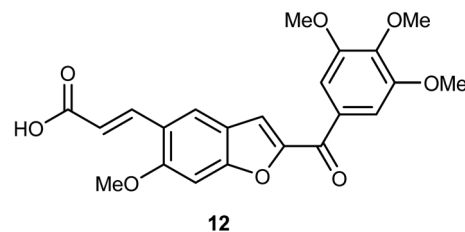
### 2.3. Anticancer activity of 2-benzoylbenzofuran derivatives

A series of 2-benzoylbenzofuran derivatives **11a–i** were synthesized and screened for *in vitro* anticancer activity against human breast cancer (MCF-7, MDA-MB-231), human embryonic kidney cancer (HEK-293), and human epidermal cancer (HaCaT) cell lines employing MTT bioassay. The benzofuran derivative **11e** demonstrated an excellent potency against anti-oestrogen receptor-dependent breast cancer cells with low toxicity, compared with the positive controls tamoxifen and raloxifene. Compound **11e** might be an interesting lead for further development as a potential inhibitor of oestrogen-receptor. Compound **11e** also significantly inhibited the growth of ER-dependent MCF-7 breast cancer cells, but had a minor effect on normal cells (HaCaT), leading to a remarkable selectivity in the treatment of breast cancer. The increased inhibitory and selectivity potency of compound **11e** were referred to its high hydrogen-bond interactions with ARG394 with a distance of  $2.9 \text{ \AA}$ .<sup>39</sup>



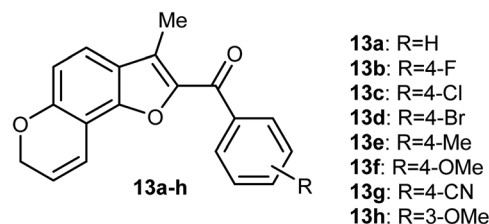
Structure of 2-benzoylbenzofurans **11a–i**

The benzofuran derivative **12** was described as a potent inhibitor against cervical cancer cells, SiHa and HeLa. Treatment with **12** enhanced the growth inhibitory rate in a concentration-dependent manner, (with  $\text{IC}_{50}$  values  $1.10$  and  $1.06 \mu\text{M}$ ) against SiHa and HeLa cells, respectively, which were higher than the positive reference combretastatin (CA-4) (with  $\text{IC}_{50}$  values  $1.76$  and  $1.86 \mu\text{M}$ ), respectively. The mechanistic studies showed that benzofuran derivative **12** induced G2/M phase arrest and apoptosis in SiHa and HeLa cells.<sup>40</sup>



Structure of the 2-benzoylbenzofuran derivative **12**

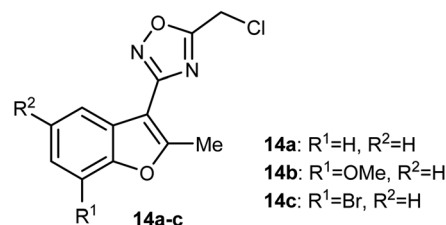
The *in vitro* antiproliferative activity of the benzofuran hybrids **13a–h** was reported by Dharavath *et al.* against two cell lines; C-6 (nerve cells) and MCF-7 (human breast adenocarcinoma cells) using the MTT method. The bioassay data of the *in vitro* antiproliferative activity disclosed that the benzofuran derivatives **13b** and **13g** demonstrated superior inhibition against MCF-7 cell line (with  $\text{IC}_{50}$   $1.875$  and  $1.287 \mu\text{M}$ , respectively), much better than the cisplatin drug ( $\text{IC}_{50}$   $2.184 \mu\text{M}$ ). Compounds **13b** and **13g** showed also excellent inhibitory activity against C-6 cell line (with  $\text{IC}_{50}$   $1.980$  and  $1.622 \mu\text{M}$ , respectively) with more potency than the standard drug cisplatin ( $\text{IC}_{50}$   $2.258 \mu\text{M}$ ). The other compounds showed moderate antiproliferative activity with  $\text{IC}_{50}$  ranging between  $2.207$ – $5.278 \mu\text{M}$  and  $2.635$ – $4.826 \mu\text{M}$  against MCF-7 and C-6 cell lines, respectively. All compounds showed strong binding interactions with calf thymus DNA (CT-DNA) through an intercalation mode when measured by UV-vis spectroscopy and fluorescence. Thus, compounds **13b** and **13g** were considered as promising candidates for further exploration of new therapeutics.<sup>41</sup>



Structure of the benzofuran hybrids **13a–h**

### 2.4. Anticancer activity of 3-oxadiazolylbenzofuran derivatives

A set of benzofuran-based oxadiazole conjugates **14a–c** were reported to have promising anticancer activities. Evaluation of the *in vitro* cytotoxic activity of compounds **14a–c** against the pancreatic cancer cells (MIA PaCa2) and human colon cancer cells (HCT116) was discussed, where the  $\text{IC}_{50}$  values ranged between  $3.27$ – $11.27$



Structure of the benzofuran-based oxadiazole derivatives **14a–c**



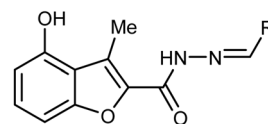
$\mu\text{M}$ . The bromo derivative **14c** was the most efficient one against HCT116 with  $\text{IC}_{50}$  value  $3.27 \mu\text{M}$ . The decrease of glycogen synthase kinase-3 $\beta$  (GSK3 $\beta$ ) induced apoptosis *via* suppression of basal NF- $\kappa\text{B}$  activity in MIA-PaCa2 and HCT116.<sup>42</sup>

## 2.5. Anticancer activity of benzofuran-2-carbohydrazone derivatives

Synthesis of 3-methylbenzofuran derivatives **16a–h** and **17a–c** and 3-(morpholinomethyl)-benzofuran derivatives **18a–e** and **19a–b** as anticancer agents towards the cell lines NCI-H23 and A549, with VEGFR-2 inhibitory potency was reported. All the benzofuran compounds greatly inhibited both the cancer cell lines NCI-H23 and A549. The 3-methylbenzofuran derivative **16b**, having *p*-methoxy group, exerted the most antiproliferative activity against A549 cell line ( $\text{IC}_{50} = 1.48 \mu\text{M}$ ) closer to the reference drug staurosporine ( $\text{IC}_{50} = 1.52 \mu\text{M}$ ). Furthermore, the benzofurans **16b**, **18a** and **18d** displayed good VEGFR-2 inhibitory activity with  $\text{IC}_{50}$  equal 77.97, 132.5 and 45.4 nM, respectively. Moreover, the three benzofurans **16b**, **18a** and **18d** had high cytotoxic impact towards normal lung WI-38 cells showing mean tumor selectivities equal 5.3, 8.4 and 12.9, respectively. A molecular docking study showed that the derivatives **16b**, **18a** and **18d** had different types of hydrophobic and hydrogen bonding interactions through their carbonyl oxygen

(C=O) and NH functions with the key ASP-1046 and GLU-885 amino acids residues.<sup>43</sup>

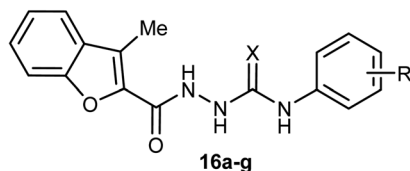
A library of benzofuran acylhydrazone scaffolds **20a–t** were reported as potent inhibitors of LSD1 (histone lysine specific demethylase 1); a therapeutic target in oncology with over-expression in several human tumors. Among the reported benzofurans, fifteen compounds demonstrated excellent inhibitory activity against LSD1 with  $\text{IC}_{50}$  varying between 3.5–



**20a–t**

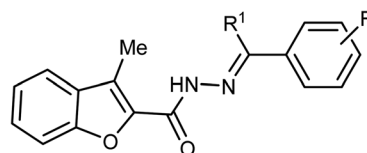
<b>20a:</b> R= Ph	<b>20k:</b> R= 3-MeOC <sub>6</sub> H <sub>4</sub>
<b>20b:</b> R= 2-furyl	<b>20l:</b> R= 2-FC <sub>6</sub> H <sub>4</sub>
<b>20c:</b> R= 2-thienyl	<b>20m:</b> R= 3-FC <sub>6</sub> H <sub>4</sub>
<b>20d:</b> R= 2-pyridyl	<b>20n:</b> R= 4-FC <sub>6</sub> H <sub>4</sub>
<b>20e:</b> R= 3-pyridyl	<b>20o:</b> R= 2-CF <sub>3</sub> C <sub>6</sub> H <sub>4</sub>
<b>20f:</b> R= 4-pyridyl	<b>20p:</b> R= 4-CF <sub>3</sub> C <sub>6</sub> H <sub>4</sub>
<b>20g:</b> R= 2-OHC <sub>6</sub> H <sub>4</sub>	<b>20q:</b> R= 2,4-(OH) <sub>2</sub> C <sub>6</sub> H <sub>3</sub>
<b>20h:</b> R= 3-OHC <sub>6</sub> H <sub>4</sub>	<b>20r:</b> R= 2-OH-6-F-C <sub>6</sub> H <sub>3</sub>
<b>20i:</b> R= 4-OHC <sub>6</sub> H <sub>4</sub>	<b>20s:</b> R= 2-OH-6-Br-C <sub>6</sub> H <sub>3</sub>
<b>20j:</b> R= 2-MeOC <sub>6</sub> H <sub>4</sub>	<b>20t:</b> R= 2-OH-5-Me-C <sub>6</sub> H <sub>3</sub>

Structure of the benzofuran-2-acylhydrazone derivatives **20a–t**



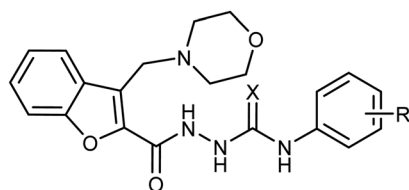
**16a–g**

<b>16a,</b> R = 3-OMe	X = S
<b>16b,</b> R = 4-OMe	X = S
<b>16c,</b> R = 3-CF <sub>3</sub>	X = S
<b>16d,</b> R = 4-F	X = S
<b>16e,</b> R = 3-OMe	X = O
<b>16f,</b> R = 4-OMe	X = O
<b>16g,</b> R = 4-Cl-3-CF <sub>3</sub>	X = O



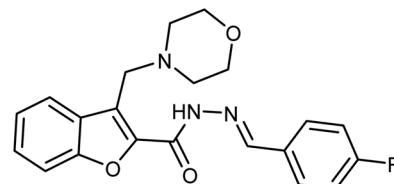
**17a–c**

<b>17a,</b> R = 3-OMe	R' = H
<b>17b,</b> R = 4-OMe	R' = H
<b>17c,</b> R = 4-OMe	R' = Me



**18a–e**

<b>18a,</b> R = 3-OMe	X = S
<b>18b,</b> R = 4-OMe	X = S
<b>18c,</b> R = 3-CF <sub>3</sub>	X = S
<b>18d,</b> R = 3-OMe	X = O
<b>18e,</b> R = 4-OMe	X = O



**19a–b**

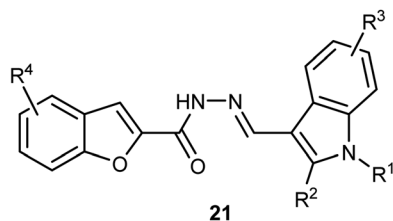
<b>19a,</b> R = H
<b>19b,</b> R = 4-OMe

Structure of the benzofuran-2-carbohydrazone derivatives **16–19**



89 nM when carried at a concentration 5  $\mu$ M. The SAR results confirmed that the compounds having two hydroxyl functions played a vital role in enhancing the inhibitory activity against LSD1 enzyme where compounds **20q**, **20r**, **20s** and **20t** had  $IC_{50}$  values in the order of 14, 15, 27 and 24 nM, respectively.<sup>44</sup>

A series of benzofuran-based hydrazide derivatives **21** were synthesized and patented by Kim *et al.* for evaluation of their antiproliferative activity using MTT method. Most of the reported hydrazides exhibited an excellent anticancer potency in a nanomolar scale ( $IC_{50}$  values ranged between 82–600 nM) with low toxicity and excellent solubility. The most potent derivative, among the reported series, against human cervical HeLa cancer cell line was the derivative **21** (where  $R^1 = CH_2CH_2CO_2Et$ ;  $R^2 = Cl$ ;  $R^3 = 5-OMe$ ;  $R^4 = 5-Me$ ) (with  $IC_{50} = 82$  nM).<sup>45</sup>

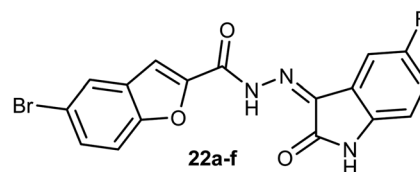


$R^1 = H, Me, -CH_2CO_2Et, -CH_2CH_2CO_2Et, -CH_2CH_2OMe$   
 $R^2 = Cl, Br, CF_3, Me$   
 $R^3 = H, 5-Me, 5-OMe, 6-OMe, 5-F, 5-Cl, 5-OCF_3$   
 $R^4 = 5-Me, 5-OMe, 5-Cl, 4,7-diMe, 4,6-diMeO, 5-NHCOMe$

#### Structure of the benzofuran hydrazide derivatives **21**

Some oxindole-based benzofuran hybrids **22a–f** were designed and synthesized as dual CDK2/GSK-3 $\beta$  inhibitors targeting breast cancer. All derivatives showed moderate to potent

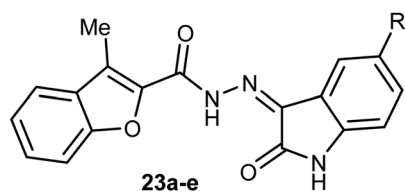
(37.77 and 52.75 nM) and (32.09 and 40.13 nM) on CDK2 and GSK-3 $\beta$ , respectively. The derivatives with the highest activity led to cell cycle arrest in the G2/M phase due to their dual CDK2/GSK-3 $\beta$  inhibition.<sup>46</sup>



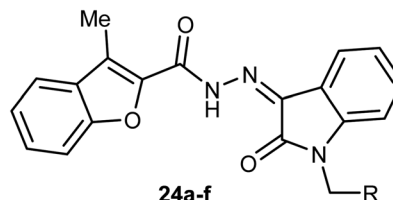
**22a**, R = H, **22b**, R = F,  
**22c**, R = Cl, **22d**, R = Br  
**22e**, R = Me, **22f**, R = OMe

#### Structure of the oxindole-based benzofuran hybrids **22a–f**

The anticancer activity of two sets of benzofuran-isatin carbohydrazide hybrids **23a–e** and **24a–f** were screened against 55 human cancer cell lines with single dose assay ( $10^{-5}$  M concentration). All derivatives **23a–e** and **24a–i** demonstrated a good anti-proliferative activity against colorectal cancer SW-620 and HT-29 cell lines. The highest the most inhibitory activity was noticed for compounds **23a** and **23d** (compound **23a** had  $IC_{50}$  values 8.7 and 9.4  $\mu$ M, and that of compound **23d** were 6.5 and 9.8  $\mu$ M, respectively). Compounds **23a** and **23d** exhibited selective cytotoxicity with a good safety study. In addition, compounds **23a** and **23d** greatly decreased the expression of the anti-apoptotic Bcl2 protein, and increased the level of the cleaved PARP and resulted in SW-620 cells apoptosis. Compounds **23a** and **23d** with such significant potency and high selective cytotoxicity suggested that they might serve as potential anticancer agents and apoptotic inducers.<sup>47</sup>



**23a**, R = H, **23b**, R = F, **23c**, R = Br  
**23d**, R = OMe, **23e**, R = NO<sub>2</sub>



**24a**, R = H, **24b**, R = Et,  
**24c**, R = CH=CH<sub>2</sub>, **24d**, R = C<sub>6</sub>H<sub>5</sub>,  
**24e**, R = 4-FC<sub>6</sub>H<sub>4</sub>, **24f**, R = 4-CNC<sub>6</sub>H<sub>4</sub>

#### Structures of the benzofuran-isatin carbohydrazides **23** and **24**

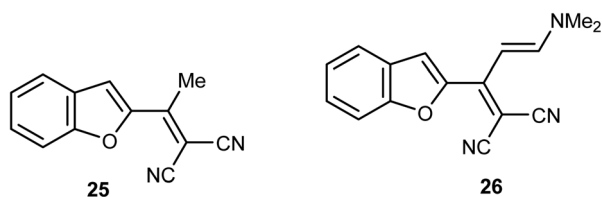
activity on both MCF-7 ( $IC_{50} = 2.27$ – $12.9$   $\mu$ M) and T-47D ( $IC_{50} = 3.82$ – $9.7$   $\mu$ M) breast cancer cell lines. Compounds **22d**, **f** were the most potent inhibitors with  $IC_{50}$  values (3.41, and 2.27  $\mu$ M) and (3.82 and 7.80  $\mu$ M) against MCF-7 and T-47D cell lines, compared with the reference drug staurosporine ( $IC_{50} = 4.81$  and 4.34  $\mu$ M), respectively. Compounds **22d**, **f** also exhibited potent dual CDK2/GSK-3 $\beta$  inhibitory activity with  $IC_{50}$  values

#### 2.6. Anticancer activity of 2-acetylbenzofuran molecular hybrids

A number of benzofuran-based hybrids **25–26** were synthesized and their *in vitro* antiproliferative activity was evaluated against HePG2, HCT-116, MCF-7, PC3, and HeLa cancer cell lines. Compounds **25** and **26** exhibited promising

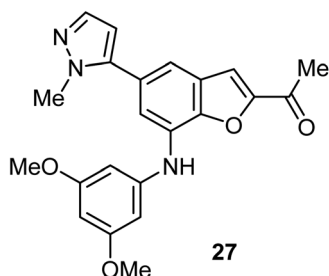


antiproliferative activity. The most active derivative **26** was then examined for its inhibition potency against EGFR kinase and the results showed that it had a remarkable EGFR TK inhibitory activity with  $IC_{50}$  value  $0.93 \mu M$ , very close to the reference drug gefitinib ( $IC_{50} = 0.9 \mu M$ ). The apoptosis results showed that compound **26** induced apoptosis of cancer cells and increased caspase-3 by 5.7-folds. Molecular docking results of **26** showed good fitting and suitable interactions with the key amino residues in the binding site of the EGFR kinase, where the cyano group enabled the hydrogen bonding interactions with the Met769 amino acid and benzofuran moiety showed van der Waals interactions with the EGFR binding site.<sup>48</sup>



Structures of the 2-acetylbenzofuran hybrids **25** and **26**

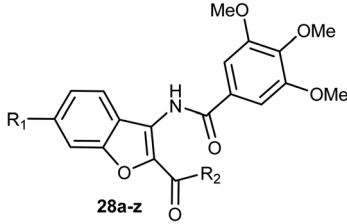
The 2-acetyl-7-phenylaminobenzofuran hybrid **27** was reported as a promising STAT3 inhibitor (signal transducer and activator of transcription 3). Interestingly, compound **27** displayed very potent antiproliferation activity against MDA-MB-468 cells with  $IC_{50}$  value of  $0.16 \mu M$ . On the other hand, compound **27** exhibited moderate to good anti-proliferation activities against HepG2, MDA-MB-231 and A549 cancer cell lines with  $IC_{50} = 1.63$ – $5.80 \mu M$ . The results proved that compound **27** caused a notable G2/M cycle-arresting and early apoptosis in a concentration-dependent manner in MDA-MB-468 cells.<sup>49</sup>



Structure of 2-acetyl-7-phenylaminobenzofuran hybrid **27**

3-Amidobenzofuran derivatives **28a–z** were synthesized and their antiproliferative activity against four cancer cell lines; HCT-116 (human colon carcinoma cells), HeLa (human cervical cancer cell), HT-29 (human colon cancer cell lines), and MDA-MB-231 (human breast cancer cell) were tested by MTT assay. Most of the benzofurans showed promising antiproliferative activity against the tested cancer cell lines. Compound **28g** was the most active inhibitor and showed significant antiproliferative efficacy toward MDA-MB-231, HCT-116, and HT-29 with  $IC_{50}$  values of  $3.01$ ,  $5.20$ , and  $9.13 \mu M$ , respectively (Table 1). The flow cytometric analysis of the cell cycle showed that **28g**

Table 1 Antiproliferative activities of compounds **28a–z** against human cancer cell lines



Comp.	R <sup>1</sup>	R <sup>2</sup>	<i>In vitro</i> cytotoxicity ( $IC_{50}$ , $\mu M$ ) <sup>a</sup>			
			HCT-116	HT-29	HeLa	MDA-MB-231
<b>28a</b>	H	Ph	>30	>30	>30	>30
<b>28b</b>	H	4-MeC <sub>6</sub> H <sub>4</sub>	3.70	13.21	>30	26.10
<b>28c</b>	H	4-BrC <sub>6</sub> H <sub>4</sub>	6.02	19.61	>30	>30
<b>28d</b>	H	4-ClC <sub>6</sub> H <sub>4</sub>	11.22	9.71	25.16	9.70
<b>28e</b>	H	4-MeOC <sub>6</sub> H <sub>4</sub>	9.01	11.64	19.70	12.15
<b>28f</b>	H	Me	>30	14.60	>30	>30
<b>28g</b>	H	4-FC <sub>6</sub> H <sub>4</sub>	5.20	9.13	11.09	3.01
<b>28h</b>	Cl	4-BrC <sub>6</sub> H <sub>4</sub>	18.20	>30	>30	29.17
<b>28i</b>	Cl	4-MeOC <sub>6</sub> H <sub>4</sub>	10.98	14.09	>30	15.06
<b>28j</b>	Cl	4-MeC <sub>6</sub> H <sub>4</sub>	20.96	19.70	>30	27.04
<b>28k</b>	Cl	4-ClC <sub>6</sub> H <sub>4</sub>	21.98	20.18	>30	>30
<b>28l</b>	Cl	Ph	>30	>30	>30	>30
<b>28m</b>	Cl	4-FC <sub>6</sub> H <sub>4</sub>	20.10	26.80	>30	24.07
<b>28n</b>	Cl	4-BrC <sub>6</sub> H <sub>4</sub>	>30	24.12	>30	>30
<b>28o</b>	Me	4-FC <sub>6</sub> H <sub>4</sub>	26.01	>30	>30	>30
<b>28p</b>	Me	4-ClC <sub>6</sub> H <sub>4</sub>	22.36	>30	>30	>30
<b>28q</b>	Me	4-BrC <sub>6</sub> H <sub>4</sub>	>30	29.02	>30	16.41
<b>28r</b>	Me	Ph	>30	>30	>30	>30
<b>28s</b>	Me	4-MeC <sub>6</sub> H <sub>4</sub>	>30	11.02	>30	12.88
<b>28t</b>	Me	4-MeOC <sub>6</sub> H <sub>4</sub>	>30	17.90	>30	20.75
<b>28u</b>	Me	4-BrC <sub>6</sub> H <sub>4</sub>	>30	10.29	>30	7.80
<b>28v</b>	MeO	4-ClC <sub>6</sub> H <sub>4</sub>	>30	17.63	>30	22.14
<b>28w</b>	MeO	4-MeOC <sub>6</sub> H <sub>4</sub>	>30	8.28	>30	16.58
<b>28x</b>	MeO	4-MeC <sub>6</sub> H <sub>4</sub>	>30	>30	>30	>30
<b>28y</b>	MeO	4-BrC <sub>6</sub> H <sub>4</sub>	>30	26.01	>30	>30
<b>28z</b>	MeO	Ph	>30	7.02	>30	>30

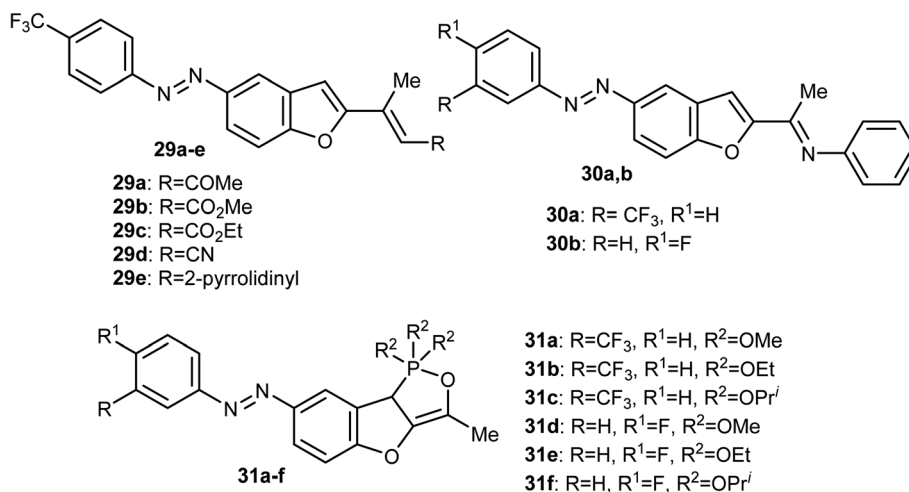
<sup>a</sup>  $IC_{50}$  values are presented as mean values of three independent experiments done in quadruplicates. Coefficients of variation were <10%.

could induce cell cycle arrest at G2/M phase in a dose-dependent manner.<sup>50</sup>

El-Sayed *et al.* discussed the synthesis and anticancer activity of the benzofuran derivatives **29**, **30** and **31**. The biological activity was assessed by evaluating their antiproliferative activities against two human cancer cell lines: MCF-7 and HepG2 cells. The benzofuran molecules **29b**, **30a**, and **31c** demonstrated the best antiproliferative potency against the two cell lines compared to the reference drug doxorubicin. The mechanism of action study revealed that derivative **30a** displayed promising inhibition of tubulin polymerization which resulted in cell cycle arrest in the G2/M phase, mitotic spindle formation disruption, and apoptosis of HepG2 cells. The benzofuran derivatives **30a**, **31c**, and **29b**, were also found to inhibit tubulin polymerization in both cell lines. Docking study established the

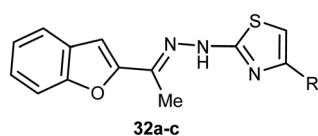




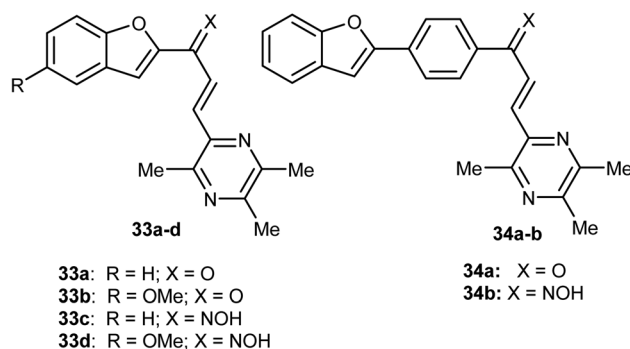
Structures of benzofuran derivatives **29**, **30** and **31**

*in vitro* results confirming that compound **30a** was a promising anticancer agent.<sup>51</sup>

El-Khouly *et al.* reported the anticancer activity of the benzofuran derivatives **32a–c** against four cancer cell lines; HePG2, HeLa, MCF-7 and PC3. The bioassay results confirmed that most of the derivatives had promising inhibitory potency against the defined cell lines with IC<sub>50</sub> values ranging between 8.49–16.72 μM, 6.55–13.14 μM and 4.0–8.99 μM, respectively, when compared with doxorubicin reference drug (4.17–8.87 μM). SAR study revealed that compound **32a**, having methyl group at thiazole scaffold, showed higher inhibition compared to all other derivatives.<sup>52</sup>

**32a**, R = Me; **32b**, R = Ph; **32c**, R = CH<sub>2</sub>CO<sub>2</sub>EtStructure of benzofuran derivatives **32**

Bukhari *et al.* reported the synthesis of some benzofuran-chalcone derivatives **33** and **34** and screened for their *in vitro* anticancer activity against A-375, MCF-7, A-549, HT-29 and H-460 human cancer cell lines. All of the synthesized benzofuran-chalcone derivatives showed good to moderate activity against all of the tested cell lines compared with cisplatin as a positive control. Compound **33d** showed the highest inhibition activity with IC<sub>50</sub> values 4.15, 3.22, 2.74, 7.29, 3.81 μM against four different cell lines; A-375, MCF-7, A-549, HT-29 and H-460, respectively, compared with cisplatin (IC<sub>50</sub> values 9.46, 12.25, 5.12, 25.4, 6.84 μM, respectively).<sup>53</sup>

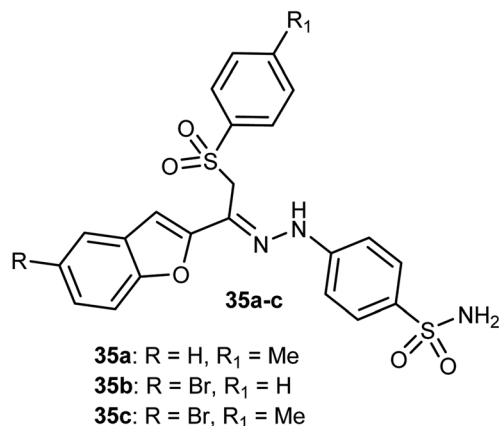
Structures of benzofuran-chalcone derivatives **33** and **34**.

The sulfonamide-arylhydrazones of benzofuran derivatives **35a–c** were tested for their inhibitory actions toward the target tumor-associated hCA-I, hCA-II, hCA-IX and XII isoforms. The reported compounds were effective inhibitors of hCA-IX and XII isoforms with K<sub>i</sub> spanning values 10.0–97.5 and 10.1–71.8 nM, respectively. They demonstrated the highest selectivity toward hCA IX and XII over hCA I (SIs: 39.4–250.3 and 26.0–149.9, respectively), and over hCA II (SIs: 19.6–57.1 and 13.0–34.2, respectively).<sup>54</sup>

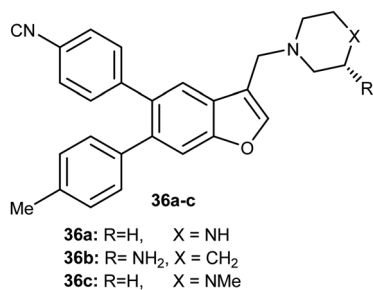
## 2.7. Anticancer activity of piperazine-based benzofuran derivatives

The benzofuran scaffolds **36** were synthesized and their inhibitory activities against LSD1 (lysine-specific demethylase-1) were examined. Compound **36b** was the most potent inhibitor of LSD1 with an IC<sub>50</sub> value 0.065 μM. Compound **36c** with methylpiperazine moiety was less potent (IC<sub>50</sub> = 0.420 μM) than **36a** (unsubstituted piperazine), showing that hydrogen-bond donor groups at R<sup>2</sup> moiety were favorable. The *in vivo* inhibitory potency of compound **36b** was evaluated at a dose of 10 and

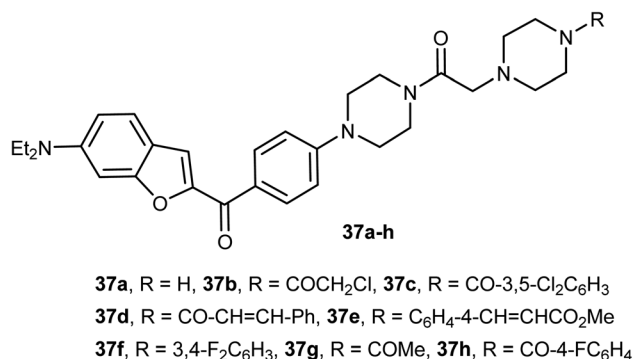


Structure of 2-(sulfonamido-arylhydrazonoacetyl)benzofuran hybrids **35**

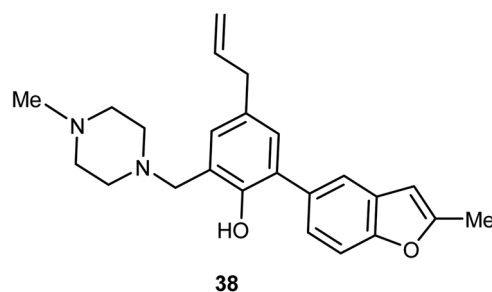
20 mg kg<sup>-1</sup> day<sup>-1</sup>, where after 15 days of treatment at a dose of 20 mg kg<sup>-1</sup> day<sup>-1</sup>, compound **36b** remarkably inhibited the tumor growth and decreased the average tumor weight and volume by 64% and 68%, respectively, in comparison with the control. All tumor studies revealed that compound **36b** was a promising lead structure, where it effectively inhibited H460 cell growth *in vivo* without significant side effects.<sup>55</sup>

Structure of piperazine-based benzofurans **36**

The piperazine-based benzofurans **37a-h** were synthesized and their *in vitro* anticancer activities were tested against five human cancer cell lines; MCF-7, A549, HeLa, HCT116 and human gastric carcinoma (SGC7901) by MTT assay. Compounds **37a-h** showed highly selective cytotoxic activity against the five cancer cells (IC<sub>50</sub> < 10 μM), better or equal to the inhibitory activity of 5-fluorouracil (5-FU). The SAR study declared that electron-donor groups on the phenyl ring (such as CH<sub>3</sub>, CH<sub>3</sub>O, Cl and F) resulted in more promising anticancer activities, however, electron-withdrawing groups (such as CN and CF<sub>3</sub>) minimized the activity. Compound **37e** demonstrated a promising anticancer activity against A549, HeLa, SGC7901, HCT116 and MCF-7 cell lines. Apoptosis study revealed that compound **37e** significantly induced apoptosis on A549 cell.<sup>56</sup>

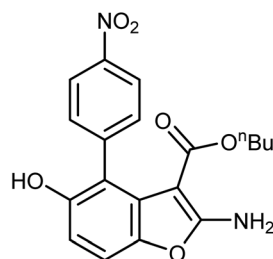
Structure of piperazine-based benzofurans **37a-h**

The piperazine-based benzofuran derivative **38** was designed, synthesized and evaluated as antitumor agent using MTT colorimetry method. Compound **38** was characterized by its high *in vitro* inhibitory activity against A549 and K562 cancer cells with IC<sub>50</sub> values of 25.15 μM and 29.66 μM, respectively. The experiment was conducted at five concentrations (ranging between 128–8 μM), and each concentration was six parallel samples in triplicates. Thus, compound **38** was useful for further development as an anticancer drug.<sup>57</sup>

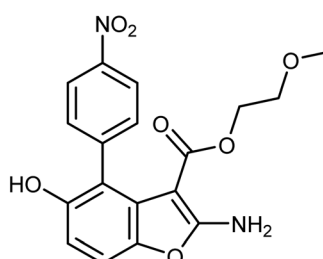
Structure of piperazine-based benzofuran **38**

## 2.8. Anticancer activity of 2-aminobenzofuran derivatives

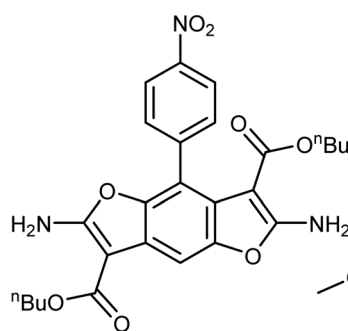
The 2-aminobenzofuran derivatives **39**, **40** and benzodifurans **41**, **42** were designed, synthesized and their anticancer potentials against prostatic tumor cells (PC-3) were evaluated. The bioassay results showed that the anticancer potential was affected by lipophilicity, where the anticancer activity of 2-aminobenzofuran derivatives was more promising when compared to benzodifurans. The benzofuran **39** was the most promising molecule. The benzofuran **39**-treatment decreased PC-3 cell viability in a dose-dependent manner with  $IC_{50} = 33 \mu M$  as determined by CCK-8 assay (cell counting kit-8).<sup>58</sup>



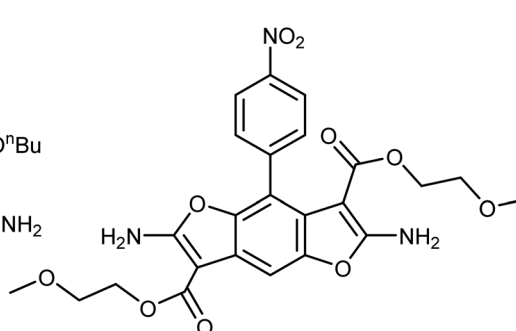
**39:** ( $IC_{50} = 33 \mu M$ )



**40:** ( $IC_{50} = 142 \mu M$ )



**41:** ( $IC_{50} = 146 \mu M$ )

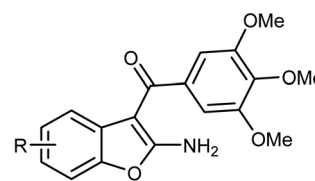


**42:** ( $IC_{50} > 200 \mu M$ )

Structures of 2-aminobenzofurans **39** and **40** and benzodifurans **41** and **42**

A series of biologically active 2-aminobenzofuran derivatives **43a–n** were synthesized and evaluated *in vivo* and *in vitro* as inhibitors of tubulin polymerization. The *in vitro* antiproliferative activities against the six human cell lines; HT-29, HL-60, HeLa, medulloblastoma (Daoy), B-cell leukemia (SEM) and T-cell leukemia (Jurkat) was examined using combretastatin A-4 (CA-4) phosphate as a reference standard. The SAR study showed that the position of electron-donating or electron-withdrawing groups at the benzene ring of benzofuran had a great effect on the inhibitory potency. The presence of 6-methoxy group on benzofuran caused the maximum inhibitory activity while the presence of 4-methoxy group caused the least inhibitory activity. A similar effect was also noticed in the case of the presence of ethoxy, methyl or bromo substituents at position-6 of benzofuran, particularly the 6-ethoxybenzofuran derivative **43f** was the most potent compound of the prepared series. The derivatives **43f** and **43l** were the most potent compounds of the series (with  $IC_{50}$  values 0.005–2.8 and 0.3–3.5 nM, respectively) against the six cancer cell lines, as compared with CA-4 (with  $IC_{50} = 0.8$ –3100 nM). More specifically,

30  $mg\ kg^{-1}$  against a syngeneic murine mammary tumor, where treatment with CA-4 reduced tumor growth by 26.5% only.<sup>59</sup>



**43a–n**

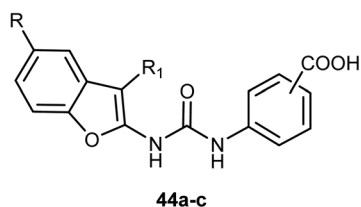
- |   |                                   |
|---|-----------------------------------|
| <b>43a:</b> R = H,  | <b>43b:</b> R = 4-OMe             |
| <b>43c:</b> R = 5-OMe,  | <b>43d:</b> R = 6-OMe             |
| <b>43e:</b> R = 7-OMe,  | <b>43f:</b> R = 6-OEt             |
| <b>43g:</b> R = 6- <i>n</i> -OC <sub>3</sub> H <sub>7</sub> , | <b>43h:</b> R = 7-OEt             |
| <b>43i:</b> R = 6-OCH <sub>2</sub> Ph,                        | <b>43j:</b> R = 6-F               |
| <b>43k:</b> R = 6-Br,   | <b>43l:</b> R = 6-Me              |
| <b>43m:</b> R = 6-OH,   | <b>43n:</b> R = 5-NH <sub>2</sub> |

Structure of 2-aminobenzofurans **43a–n**

Benzofuran-based carboxylic acids **44a–c** were evaluated for their anti-proliferative action against human breast cancer



(MCF-7 and MDA-MB-231) cell lines. The derivatives showed variable inhibitions towards MCF-7 and MDA-MB-231 cell lines. In particular, the benzofuran derivative **44b** was the most effective toward MDA-MB-231 ( $IC_{50} = 2.52 \mu M$ ) with close potency to the reference drug doxorubicin ( $IC_{50} = 2.36 \mu M$ ). The derivative **44b** (which treated MDA-MB-231 cells) was remarkably arrested at the G2-M phase by increasing the cell population to 32.30% compared to 10.80% (for control). The number of cells in the sub-G1 phase was altered to 25.53% (for **44b**-treated MDA-MB-231 cells) compared with 1.43% (for the control cells).<sup>60</sup>



Comp.	R	R <sub>1</sub>	CO <sub>2</sub> H	IC <sub>50</sub> (μM)	
				MCF-7	MDA-MB-231
<b>44a</b>	H	Me	<i>m</i>	-	37.60
<b>44b</b>	Br	H	<i>m</i>	4.91	2.52
<b>44c</b>	Br	H	<i>p</i>	19.70	11.50

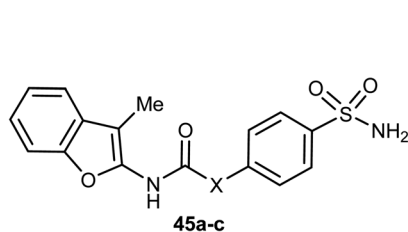
Structure of benzofuran-based carboxylic acids **44a-c**

Different series of benzofuran-based sulfonamides **45**, **46**, **47** and **48** were designed, synthesized, and were found to be potent inhibitors against four tumor-related human-carbonic

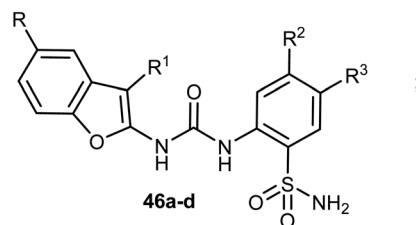
anhydrase (hCA) isoforms; hCA I, II, IX and XII. The bioassay results showed that most of the derivatives showed moderate to high inhibitory activity and in particular compounds **47b** and **47d** were the most effective hCA-IX inhibitors (with inhibition constants  $K_{is} = 8.4$  and  $5.5$  nM, respectively), and were significantly selective toward hCA-IX isoform over the off-target hCA II isoform (S. I. = 26.4 and 58.9, respectively). The antiproliferative activity of **47b** and **47d** towards two breast cancer cell lines; MDA-MB-231 and MCF-7, was measured using MTT bioassay and staurosporine as the reference drug. The biological results proved that **47b** had excellent antiproliferative activity against both cancer cell lines; MDA-MB-231 and MCF-7 (with  $IC_{50} = 6.27$  and  $6.45 \mu M$ , respectively), very close to staurosporine ( $IC_{50} = 6.75$  and  $3.67 \mu M$ , respectively), however, compound **47d** had moderate anti-proliferation action against MDA-MB-231 and MCF-7 cancer cell lines (with  $IC_{50} = 14.16$  and  $13.79 \mu M$ , respectively). In addition, the up-regulation of the expression levels of pro-apoptotic Bax and Caspase-3 proteins and down-regulation of the expression level of anti-apoptotic Bcl-2 protein were reported upon treatment of both MDA-MB-231 and MCF-7 cells with compound **47b**.<sup>61</sup>

## 2.9. Anticancer activity of benzofuran-2-carboxamide derivatives

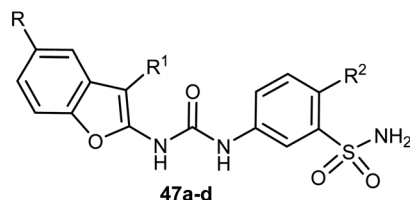
Two sets of the 1-(benzofuran-3-yl)-1*H*-1,2,3-triazole derivatives **49a-i** and **50a-i** were synthesized, and their antiproliferative activities were screened against four cancer cell lines; HCT116, HeLa, HepG2, and A549 cells. The benzofuran-2-carboxamide derivative **50g** showed the highest anti-proliferation potency against HCT-116, HeLa, HepG2, and A549 cells ( $IC_{50} = 0.87$ ,



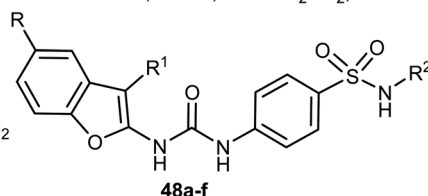
**45a:** X = O  
**45b:** X = (CH<sub>2</sub>)<sub>2</sub>  
**45c:** X = NHNHCO



**46a:** R = H, R<sup>1</sup> = Me, R<sup>2</sup> = H, R<sup>3</sup> = H  
**46b:** R = H, R<sup>1</sup> = Me, R<sup>2</sup> = SO<sub>2</sub>NH<sub>2</sub>, R<sup>3</sup> = Cl  
**46c:** R = Br, R<sup>1</sup> = H, R<sup>2</sup> = H, R<sup>3</sup> = H  
**46d:** R = Br, R<sup>1</sup> = H, R<sup>2</sup> = SO<sub>2</sub>NH<sub>2</sub>, R<sup>3</sup> = Cl



**47a:** R = H, R<sup>1</sup> = Me, R<sup>2</sup> = H  
**47b:** R = H, R<sup>1</sup> = Me, R<sup>2</sup> = Me  
**47c:** R = Br, R<sup>1</sup> = H, R<sup>2</sup> = H  
**47d:** R = Br, R<sup>1</sup> = H, R<sup>2</sup> = Me



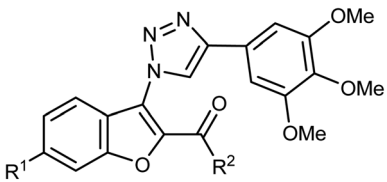
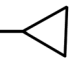
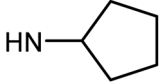
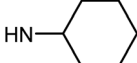
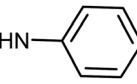

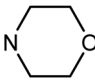
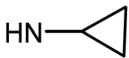
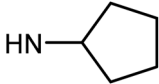
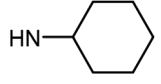
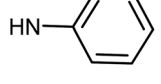
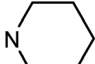
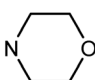
**48a:** R = H, R<sup>1</sup> = Me, R<sup>2</sup> = H  
**48b:** R = H, R<sup>1</sup> = Me, R<sup>2</sup> = 2-thiazolyl  
**48c:** R = H, R<sup>1</sup> = Me, R<sup>2</sup> = 3,4-diMe-5-isoxazolyl  
**48d:** R = Br, R<sup>1</sup> = H, R<sup>2</sup> = H  
**48e:** R = Br, R<sup>1</sup> = H, R<sup>2</sup> = 2-thiazolyl  
**48f:** R = Br, R<sup>1</sup> = H, R<sup>2</sup> = 3,4-diMe-5-isoxazolyl

Structures of benzofuran-based sulfonamides **45**, **46**, **47** and **48**





Table 2 Antiproliferative activities of compounds 49a–i and 50a–i

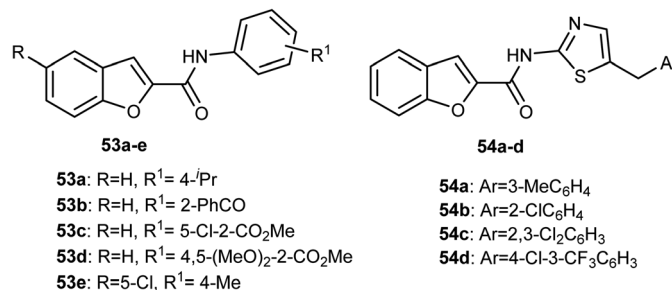
 49a-i, 50a-i						
Comp.	R <sup>1</sup>	R <sup>2</sup>	(IC <sub>50</sub> , μM) <sup>a,b</sup>			
			HCT-116	HeLa	HepG2	A549
49a	H	OEt	>100	>100	30.97 ± 6.24	>100
49b	H	OCH(CH <sub>3</sub> ) <sub>2</sub>	41.71 ± 8.94	59.30 ± 5.15	58.00 ± 9.48	>100
49c	H	HN(CH <sub>2</sub> ) <sub>2</sub> CH <sub>3</sub>	16.43 ± 4.19	6.84 ± 0.34	2.92 ± 0.22	9.29 ± 3.66
49d	H	HN- 	>100	>100	>100	>100
49e	H	HN- 	6.07 ± 0.38	43.37 ± 7.55	36.82 ± 5.43	22.52 ± 2.65
49f	H	HN- 	8.59 ± 5.47	24.99 ± 7.71	51.12 ± 9.75	94.74 ± 8.93
49g	H	HN- 	1.02 ± 0.31	1.83 ± 0.52	8.34 ± 2.53	0.83 ± 0.34
49h	H	N- 	73.52 ± 17.17	>100	65.23 ± 5.42	73.99 ± 7.86
49i	H	N- 	>100	>100	64.85 ± 2.98	>100
50a	OMe	OEt	36.64 ± 7.30	>100	11.57 ± 3.59	>100
50b	OMe	OCH(CH <sub>3</sub> ) <sub>2</sub>	40.21 ± 4.23	29.48 ± 0.67	14.79 ± 5.02	50.41 ± 7.88
50c	OMe	HN(CH <sub>2</sub> ) <sub>2</sub> CH <sub>3</sub>	52.46 ± 8.74	2.84 ± 0.95	6.29 ± 2.93	>100
50d	OMe	HN- 	>100	78.38 ± 7.48	>100	>100
50e	OMe	HN- 	1.27 ± 0.38	7.66 ± 1.26	20.26 ± 9.05	18.95 ± 3.17
50f	OMe	HN- 	5.56 ± 1.76	29.99 ± 5.59	41.65 ± 6.01	>100
50g	OMe	HN- 	0.87 ± 0.79	0.73 ± 0.67	5.74 ± 1.21	<b>0.57 ± 0.31</b>
50h	OMe	N- 	47.79 ± 7.56	>100	6.83 ± 3.21	38.79 ± 16.90
50i	OMe	N- 	80.08 ± 0.86	49.75 ± 11.74	10.92 ± 4.65	37.85 ± 6.96

<sup>a</sup> IC<sub>50</sub> values are presented as the means ± SD of triplicate experiments. <sup>b</sup> Drug treatment for 72 h.

0.73, 5.74 and 0.57  $\mu\text{M}$ , respectively) (Table 2). The SAR study proved that the presence of 6-methoxy group (as in structures **50a–i**) was essential for high antiproliferative activity compared with the unsubstituted analogues **49a–i**. The mechanistic studies demonstrated that compound **50g** diminished the polymerization of tubulin, resulting in disruption of mitotic spindle formation, cell cycle arrest in the G2/M phase, and apoptosis of A549 cells. Thus, compound **50g** was worthy to be a lead compound of further development as an anticancer agent.<sup>62</sup>

The benzofuran-carboxamide derivatives **51a–j** and **52a–d** were synthesized and their antiproliferative activities were conducted against four human cancer cell lines; HT-29, MCF-7, Panc-1 and epithelial cancer (A-549) using MTT assay method and doxorubicin as a reference drug. Some compounds exhibited good antiproliferative activities against the cancer cells and the 4-(morpholin-4-yl)phenethyl derivative **51d** was the most active one against all of the four cell lines (with  $\text{IC}_{50}$  values ranging between 0.70–1.8  $\mu\text{M}$ ), with almost equal potency to doxorubicin reference (with  $\text{IC}_{50}$  values ranging between 0.90–1.41  $\mu\text{M}$ ). The most active caspase-3 enhancers were compounds **51d** and **51h** which led to an increase in the levels of caspase 8 and 9 declaring activation of both intrinsic and extrinsic pathways. Both compounds **51d** and **51h** showed marked induction of Bax, and down-regulation of Bcl-2 protein levels in MCF-7 cell lines. Compound **51d** also demonstrated cell cycle arrest at the Pre-G1 and G2/M phases in the cell cycle of MCF-7 cell line. The SAR analysis revealed that the presence of the *N*-phenethyl carboxamide moiety considerably improved the antiproliferative activity of compounds **51** and such activity was further enhanced by the presence of a morpholinyl group at the *para*-position of the *N*-phenethyl ring causing compound **51d** to have antiproliferative activity similar to the reference drug doxorubicin. In addition, the effect of *para* substitution at the phenethyl moiety on the antiproliferative activity of compounds **51** was in the order: morpholinyl > piperidinyl  $\geq$  pyrrolidinyl > dimethylamino > H.<sup>63</sup>

The *in vitro* anticancer activity of the benzofuran-carboxamides **53** and **54** were screened by Matiichuk *et al.*

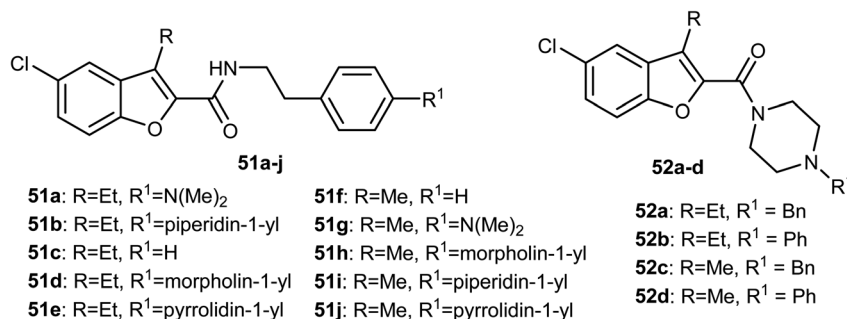


Structures of benzofuran-carboxamides **53** and **54**

against sixty human tumor cell lines obtained from nine neoplastic diseases. The results showed that all of the tested compounds displayed different levels of activity. The mean graph mid-points (MG-MID) were determined for  $\text{GI}_{50}$  and TGI (TGI is the molar concentration of a compound leading to total inhibition), to get an average activity factor over all cell lines for the tested compound. Compound **54a** disclosed high inhibition potency ( $\text{GI}_{50} < 10 \mu\text{M}$ ) against all of the 58 tested tumor cell lines (with MG-MID = 2.03  $\mu\text{M}$ ), **54c** showed high inhibition potency against 56 cell lines (MG-MID = 3.26  $\mu\text{M}$ ) and **54d** exhibited high inhibition potency against 53 human tumor cell lines (MG-MID = 3.26  $\mu\text{M}$ ). The colon cancer subpanel exhibited the best sensitivity to compounds **54a** and **54c** (with a mean  $\text{GI}_{50} = 0.87$  and 0.84  $\mu\text{M}$ , respectively). The most sensitive cell line was T-47D (Breast Cancer,  $\text{GI}_{50} = 0.088 \mu\text{M}$ ). In contrast, compounds **53a–e** showed weak to moderate activity on the tested cell lines.<sup>64</sup>

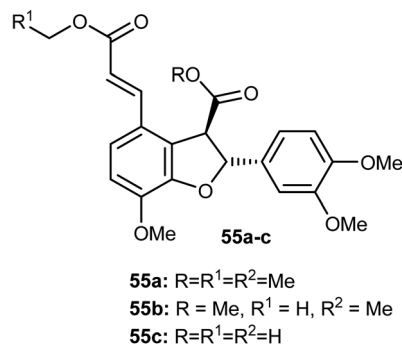
## 2.10. Anticancer activity of dihydrobenzofuran derivatives

The naturally isolated benzofuran derivatives **55a–c** (isolated from the ethyl acetate fraction of *Polygonum barbatum* weed) were examined for their anticancer potency against lung cancer



Structures of the benzofuran-carboxamide derivatives **51** and **52**

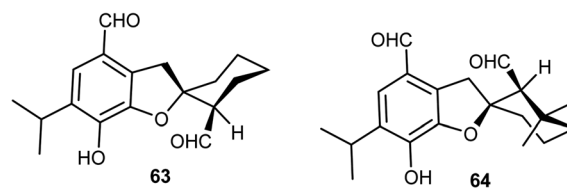
(NCI-H460) and oral cancer (CAL-27) cell lines, employing MTT assay. Compound **55a** had more anticancer potency with  $IC_{50}$  of 53.24 and 48.52  $\mu M$  against NCI-H460 and CAL-27, respectively, when compared with the standard drug 5-fluorouracil ( $IC_{50}$  = 97.76  $\mu M$ ). Compound **55a** induced apoptosis after 24–48 h treatment as confirmed by morphological and flow cytometry analysis.<sup>65</sup>



Structure of naturally isolated benzofurans **55**

Some benzofuran derivatives **56–62** were isolated from the seeds of *Psoralea corylifolia* and were screened for *in vitro* inhibitory activity against the human colon cancer (SW620) cell line. Compounds **56–62** were found to have reasonable cytotoxicity against the SW620 cells with  $IC_{50}$  = 24.31–28.72  $\mu M$  compared with 5-fluorouracil ( $IC_{50}$  = 3.19  $\mu M$ ). Among these compounds, **56** was the most cytotoxic one but compounds **59–62** did not exhibit cytotoxicity toward the SW620 cell line.<sup>66</sup>

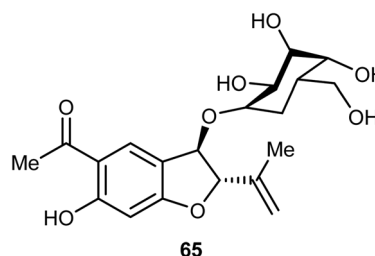
The naturally extracted spiro[benzofuran-2,1'-cyclohexane] scaffolds **63–64**, were screened for their cytotoxicity against five cancer cell lines (A-549, SMMC-7721, HL-60, MCF-7, and SW-480) and a noncancerous (BEAS-2B) cell lines. The bioassay was measured using the MTS (3-(4,5-dimethylthiazol-2-yl)-5-(3-carboxymethoxyphenyl)-2-(4-sulfophenyl)-2H-tetrazolium) method, where compound **63** exhibited significant cytotoxicity against A-549, SMMC-7721, and MCF-7 cell lines (with  $IC_{50}$



Structures of naturally spiro[benzofuran-2,1'-cyclohexanes] **63** and **64**

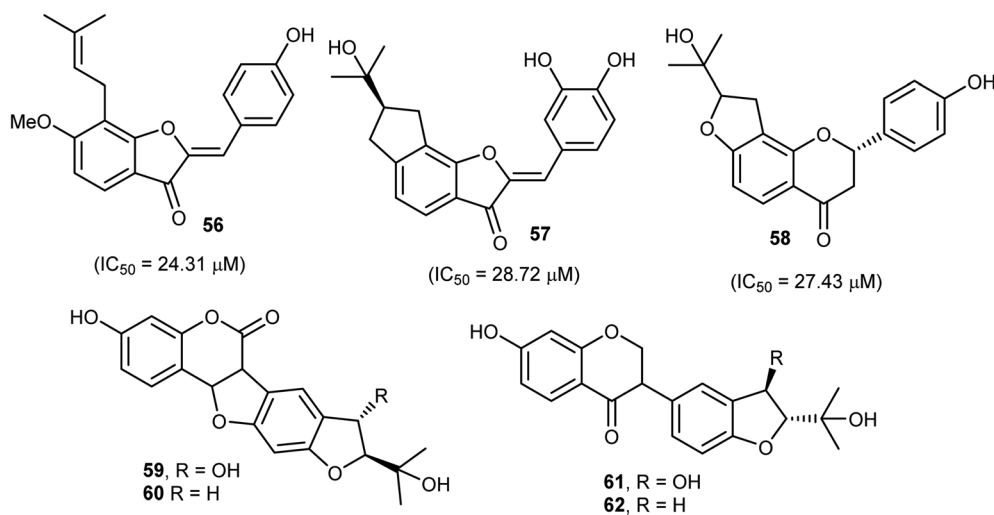
values 6.60, 7.13, and 11.50  $\mu M$ ) more potent than the reference cisplatin (13.84, 7.82, 13.46  $\mu M$ , respectively).<sup>67</sup>

The naturally benzofuran-glucoside derivative **65** was isolated from *Senecio glaucus* L. by Zaher *et al.* and evaluated for its cytotoxic activity. Compound **65** exhibited potent cytotoxic activity against the pancreatic cancer cell line (PANC-1) under glucose deficient medium ( $IC_{50}$  = 7.5  $\mu M$ ) using antimycin as anticancer reference compound.<sup>68</sup>



Structure of naturally benzofuran-glucosides **65**

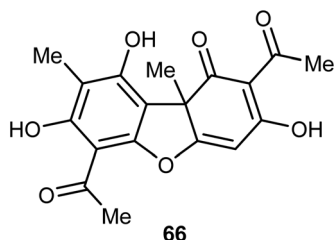
The natural product usnic acid (UA) **66** was reported as a potent anticancer agent against human gastric adenocarcinoma (AGS), gastric carcinoma (SNU-1) and squamous carcinoma (A-431) cells. The bioassay study was carried out by treatment of AGS cells with 10–50  $\mu M$  of UA in DMSO for 12, 24 and 48 h using MTT technique. UA promoted cell death in A-431 cells with  $IC_{50}$  values 98 and 39  $\mu M$  after 48 and 72 h of UA treatment, respectively. UA reduced the cell viability of AGS cells by 17–45%, 20–65%, and 52–80% ( $P < 0.05$ – $0.001$ ) after 12, 24, 48 h, respectively. On the other hand, UA treatment had no remarkable effect on the cell viability



Structure of naturally isolated benzofurans **56–62**



of human HaCaT and HEK-293 cells after 48 h. Thus, UA induced cytotoxic effects on human gastric cancer cells but not on normal gastric cells. Furthermore, UA **66** demonstrated selective apoptotic effect (10–25  $\mu\text{M}$ ) through the generation of ROS and led to DNA damage on human gastric cancer cells accompanied by upregulation of  $\gamma\text{H2A.X}$  (Ser139) phosphorylation, DNA-PKcs and p53.<sup>69,70</sup>

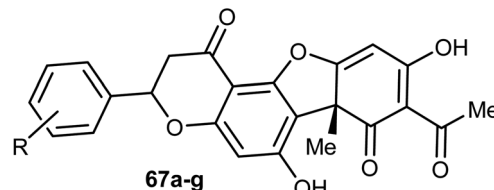


Structure of usnic acid (UA) **66**

Usnic acid (UA) **66** encapsulated heparin-modified gellan gum (HAG) nanoparticles (NPs) was synthesized and its *in vitro* cytotoxicity screening against human lung cancer cell line A549 was performed using SRB bioassay. The  $\text{IC}_{50}$  values were 12 and 14  $\mu\text{M}$  for the free and encapsulated forms of usnic acid, respectively. The *in vitro* cytotoxicity study, apoptosis assay and cell cycle assay determined that the developed nanoparticulate formulation was safe and effective and that the HAG NPs were more suitable for inhibition of cancer cell growth and as a drug delivery carrier than the free form of the drug.<sup>71</sup>

Wang *et al.* reported the synthesis and anticancer activity of some usnic acid (UA) derivatives **67a–g** against leukemia cells using (+)-UA parent compound as a positive control. The biological assay revealed that the UA-derivatives **67a–g** inhibited the proliferation of the leukemia cells; HL-60 and K562 with  $\text{IC}_{50}$  ranging between 2.15–3.25 and 2.70–6.20  $\mu\text{M}$ , respectively. Particularly, the 4-fluoro and 4-chloro substituted derivatives **67c** and **67g** exhibited the highest potency against both cells HL-

60 and K562 with  $\text{IC}_{50} = 2.64\text{--}2.82\ \mu\text{M}$ . The mechanism of the study proved that compound **67g** induced apoptosis in HL-60 and K562 cell lines, and affected the expression of MNK/eIF4E axis-related proteins, such as Mcl-1, p-eIF4E, p-4E-BP1. The bioassay results confirmed that **67g** was a potent apoptosis inducer in leukemia cells, where compound **67g** caused significant apoptosis occurrence in HL-60 cells at 6  $\mu\text{M}$  (63.5%) in comparison with control cells (2.6%). In contrast, K562 cells were less sensitive to **67g**, and the apoptosis was observed at a prolonged period at 48 h and higher concentrations.<sup>72</sup>

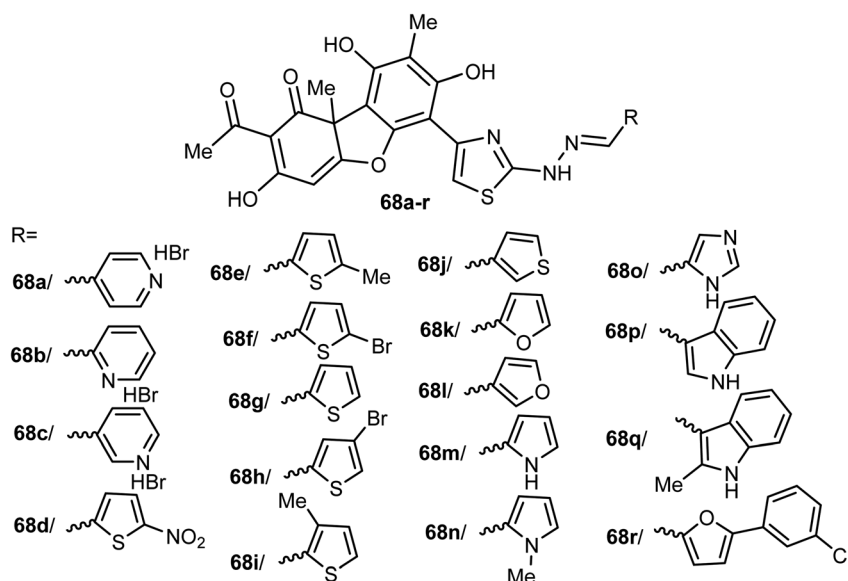


**67a**, R = H; **67b**, R = 3- $\text{NO}_2$ ; **67c**, R = 4-F; **67d**, R = 4-MeO; **67e**, R = 4-Br; **67f**, R = 3-Cl; **67g**, R = 4-Cl

Structure of usnic acid derivatives **67**

A new series of the usnic acid derivatives **68a–r** having hydrazonothiazole pharmacophores were described and tested as Tdp1 inhibitors. Most of the prepared compounds were found to have high inhibitory potency with  $\text{IC}_{50}$  values in a nanomolar scale ( $\text{IC}_{50} = 20\text{--}200\ \text{nM}$ ). The SAR study confirmed that the size of the heterocyclic moiety and the nature of heteroatom had no significant effect on the inhibitory activity, however, the presence of a bromine atom or bulky aromatic motif attached to the heterocyclic moiety **68f–h** and **68r** enhanced the inhibitory activity. The presence of pyrrole moiety led to the most potent inhibition such as in compounds **68m** and **68n**.<sup>73</sup>

Pyrzack-Felczykowska *et al.* reported the synthesis of the usnic acid-isoxazole derivative **69** and assessed its activity

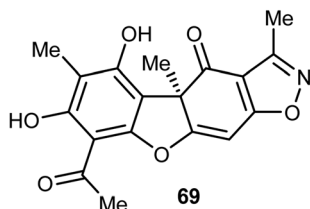


Structure of thiazole-based usnic acid derivatives **68**



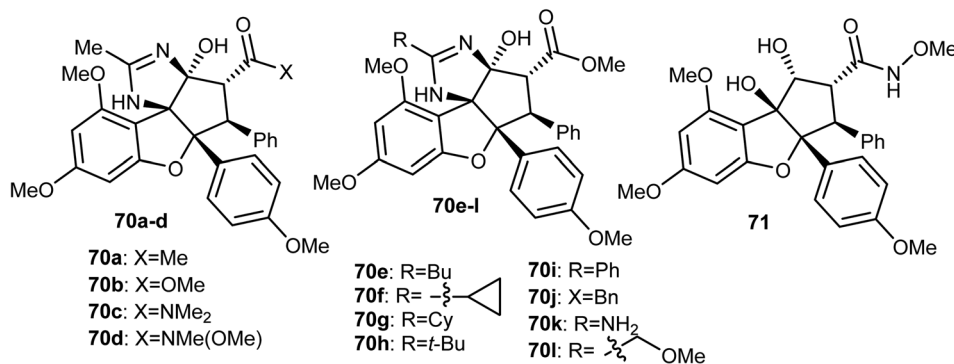


against cancer cells of different origins. The viability of breast cancer or normal cells was evaluated by MTT method. The *in vivo* anticancer activity was also examined using the mice xenograft technique. Compound **69** inhibited tumor growth upon injection to nude mice with xenografted breast cancer cells and vacuolization was selectively noticed in tumor cells but not in other organs. Thus, compound **69** induced Endoplasmic Reticulum (ER) stress in breast cancer cells but not in healthy cells. Compound **69** also effectively stopped tumor growth *in vivo*.<sup>74</sup>



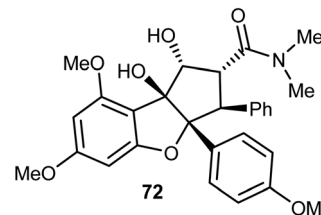
Structure of usnic acid-isoxazole derivative **69**

The anticancer activity of the amidino-rocaglates **70a-l** against MDA-MB-231 breast cancer cells was evaluated in a sulforhodamine B (SRB) assay. The benzofuran derivatives **70c**, **70d**, and **70l** were the most inhibitory active compared with the reference rocaglate-hydroxamate **71**. Compound **70d** was found to have excellent cytotoxicity with  $IC_{50} = 0.97$  nM, an almost a 2-fold increase in potency over the lead compound **71** ( $IC_{50} = 1.9$  nM). Furthermore, the dimethylamide **60c** and methyl ester **70l** were found to have  $IC_{50}$  values 1.2 and 3.6 nM, respectively. The bioassay results disclosed that amidino-rocaglates might be valuable cancer chemotherapeutic agents.<sup>75,76</sup>



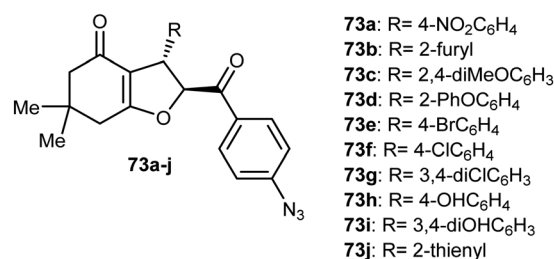
Structure of amidino-rocaglates dihydrobenzofuran derivatives **70a-l** and **71**

The natural benzofuran product (rocaglamide) **72** was reported to significantly promote the natural killer (NK) infiltration of the non-small cell lung cancer (NSCLC) cells by autophagy inhibition. Compound **72** specifically damaged mtDNA, then enhanced mtDNA leakage into the cytoplasm and activated the cGAS-STING signaling, resulting in increased infiltration of NK cells and enhanced antitumor immunity in NSCLC. Thus, compound **72** had significant potential in cancer immunotherapy.<sup>77</sup>



Structure of naturally benzofuran derivative (rocaglamide) **72**

A number of *p*-azidobenzoyl-tetrahydrobenzofuran-4(5*H*)-one hybrids **73a-j** were described by Pandit *et al.* for anticancer activity against renal cancer panel UO-31 cell lines. The results of the anticancer evaluation of the hybrids **73a-j** showed promising responses against UO-31 cell lines (<80%). The type of substituents at the phenyl moiety had a crucial effect on the activity of the compounds. Compounds **73a** and **73e**, having electron-withdrawing functions (4-NO<sub>2</sub> and 4-Br, respectively) effectively reduced the viability percentage of UO-31 cells at 10  $\mu$ M concentrations and resulted in the highest potency against UO-31 cell lines in renal cancer panel. Compounds **73a** and **73e**



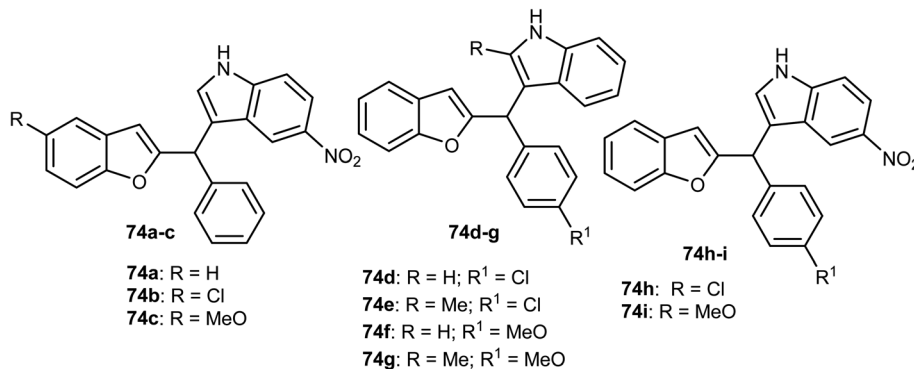
Structure of *p*-azidobenzoyl-tetrahydrobenzofuran hybrids **73**

showed high anticancer activity and prominent selectivity against UO-31 with growth inhibition of 69.36% and 80.66%, respectively.<sup>78</sup>

## 2.11. Anticancer activity of indole-based benzofuran derivatives

The anticancer activity of various indole-based benzofuran scaffolds **74a-i** were determined against two cervical cancer cell



Structures of indole-based benzofuran scaffolds **74**

lines; SiHa and C33a. Four of the prepared derivatives (**74a**, **74d**, **74e** and **74h**) demonstrated IC<sub>50</sub> values < 40 μM. Compounds **74e** and **74h** were found to be the most effective and induced autophagy as established by the progressive conversion of LC3I to LC3II and down-regulation of p62 in cervical cancer cells C33a and SiHa.<sup>79</sup>

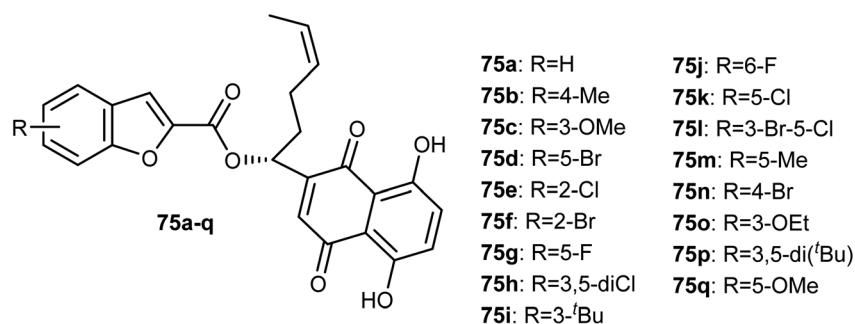
## 2.12. Anticancer activity of benzofuran-2-carboxylate derivatives

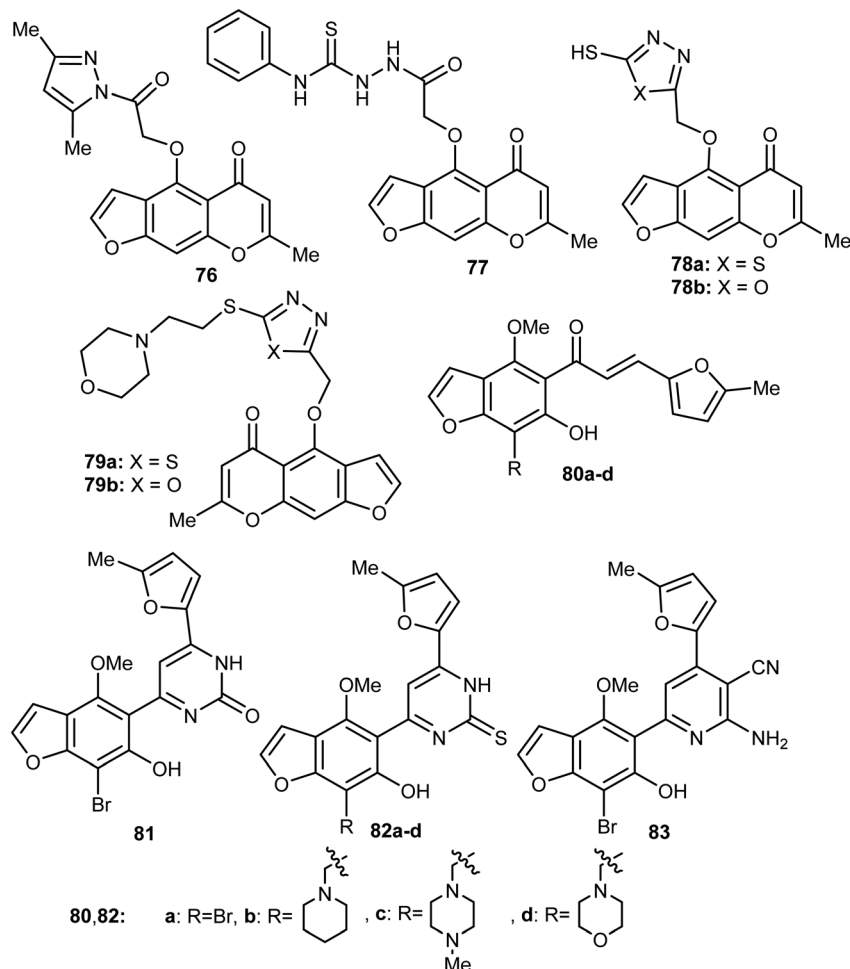
The antiproliferative activities of a number of shikonin-benzofuran substrates **75a–q** against five cancer cell lines; MDA-MB-231, HepG2, HT29, HCT116 and A549 using the MTT assay and shikonin and colchicine as the positive drugs were evaluated by Shao *et al.* Many of the reported compounds exhibited promising antiproliferation activities against the cancer cell lines compared to that of shikonin and had low cytotoxicity to non-cancer cells. Particularly, compounds **75c**, **75f** and **75i** (IC<sub>50</sub> = 0.18, 1.03 and 0.82 μM, respectively) demonstrated much higher antiproliferation potency against HT29 cells than the standard drugs, shikonin (IC<sub>50</sub> = 2.80 μM) and colchicine (IC<sub>50</sub> = 1.81 μM). The most powerful inhibition was observed for compound **75c** (IC<sub>50</sub> = 0.18 μM) against HT29 cells. Compound **75c** induced cell apoptosis, regulated the

expression of apoptosis-related proteins in HT29 cells and stimulated the HT29 cell cycle arrest at G2/M phase.<sup>80</sup>

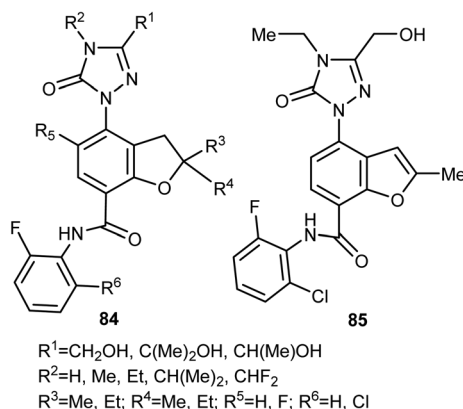
## 2.13. Anticancer activity of 4(5)-hetaryl-benzofuran derivatives

Synthesis of a large number of benzofuran derivatives **76–79** and **80–83** and their *in vitro* anticancer activity against the breast cancer cell lines; MCF-7 and MDA231 were reported. Most of the reported compounds demonstrated very potent antiproliferative activities (IC<sub>50</sub> = 1.19–2.78 μM) against MCF-7 much better than lapatinib reference drug (IC<sub>50</sub> = 4.69 μM). Moreover, the derivatives **80a** and **83** exhibited promising cytotoxic activity against both MCF-7 and MDA231. The inhibitory potencies of the derivatives **80a** and **83** against p38α MAP kinase were also highly significant with IC<sub>50</sub> = 0.04 μM superior to the reference standard SB203580 (IC<sub>50</sub> = 0.50 μM). In addition, the behavior of the benzofuran derivative **83** on the apoptotic induction and cell cycle progression of MCF-7 cell line was found to induce preG1 apoptosis and cell growth arrest at G2/M phase preventing the mitotic cycle. Compound **83** also exhibited very good drug-like properties, good ADME (absorption, distribution, metabolism and excretion) properties with moderate solubility, high GI permeation and very good bioavailability scores.<sup>81</sup>

Structure of shikonin-benzofuran substrates **75a–q**

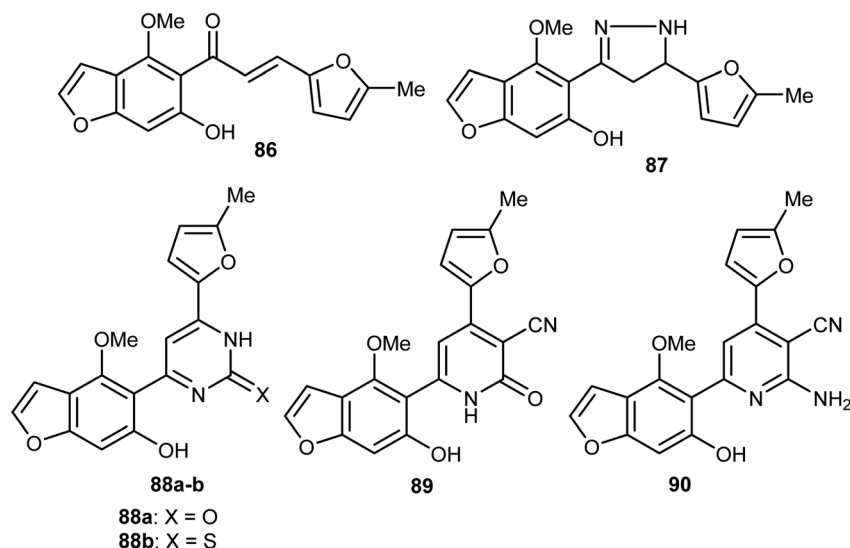
Structure of the benzofuran derivatives **76-83**

A series of dihydrobenzofuran hybrids **84** and the benzofuran derivative **85** were invented and patented by Kuduk *et al.* and then evaluated for *in vitro* inhibition of human leukemia cell line MOLM-13. The reported compounds exhibited

Structures of the dihydrobenzofuran **84** and benzofuran **85** hybrids

moderate to high inhibition effect against MOLM-13 in nanomolar scale with  $\text{IC}_{50}$  values ranging from 0.3–700 nM. Among them, four derivatives had the highest potency with  $\text{IC}_{50} = 0.3$ –7 nM. The best anti-leukemia cancer substrate was found to be compound **84** ( $R^1 = \text{C}(\text{OH})\text{Me}_2$ ,  $R^2 = \text{Me}$ ,  $R^3 = R^4 = \text{Me}$ ,  $R^5 = \text{F}$ ,  $R^6 = \text{Cl}$ ) with  $\text{IC}_{50} = 0.3$  nM, suggesting that this candidate could be further developed as anti-leukemia cancer agent.<sup>82</sup>

Ahmed *et al.* reported the synthesis of a set of benzofuran hybrids **87-90**, from the chalcone derivative **86**, and assessed their antitumor activities against breast cancer. The *in vitro* and *in vivo* bioassay results disclosed that the derivatives **86**, **88a**, and **89** revealed the highest antiproliferative activities against the MCF-7 cell line with  $\text{IC}_{50}$  values 0.07, 2.94, and 2.48  $\mu\text{M}$ , respectively, compared with the standard lapatinib ( $\text{IC}_{50} = 4.69$   $\mu\text{M}$ ). Particularly, the benzofuran molecule **86** ( $\text{IC}_{50} = 0.07$   $\mu\text{M}$ ), presented the most cytotoxic potency against MCF-7 BC cell line, caused inhibition of a panel of 22 kinases in the range of –39% to –97%, and arrested cell cycle at G2/M phase. In addition, for the *in vivo* experiments, where male swiss mice were selected as the animal model to induce solid ehrlich tumor, compound **86** reduced the tumor cells in sections of



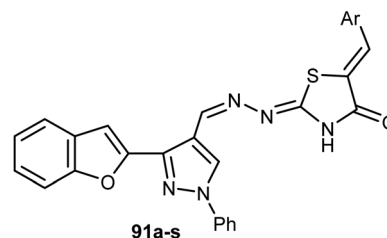
Structures of the benzofuran hybrids 87-90

ehrlich tumor, displayed a strong positive caspase-3 and negative EGFR immuno-reaction.<sup>83</sup>

#### 2.14. Anticancer activity of thiazole-based benzofuran derivatives

A set of 2-(pyrazolyl)benzofuran derivatives **91a-s** were designed, synthesized and evaluated for antiproliferative action against HeLa cell line of EGFR PK inhibitory potency. Seven compounds **91c**, **91d**, **91h**, **91j**, **91k**, **91m** and **91n** demonstrated promising sensitivity against the cancer cells. They were more potent or equipotent to the reference drug doxorubicin. For example, the derivative **91m** was the most potent anticancer agent with  $IC_{50}$  value 0.60  $\mu$ M, which was twice that of the reference drug doxorubicin ( $IC_{50}$  = 1.10  $\mu$ M). The EGFR protein kinase inhibitory activity of the synthesized compounds showed that compound **91k** was the most active one and had higher EGFR PK inhibitory activity ( $IC_{50}$  = 0.07  $\mu$ M) than that of the reference drug erlotinib ( $IC_{50}$  = 0.08  $\mu$ M). In addition, cell cycle analysis and apoptosis assay of compound **91k** were performed and it caused G1/S phase arrest and apoptosis in HeLa cancer cells, in addition to its activation of the caspases-7 and -3. The molecular docking study showed that compound **91k** had a good fitting and proper interaction with the key amino residues in the binding site of EGFR kinase compared to erlotinib. SAR study revealed that electron-withdrawing substituents at the benzylidene moiety greatly affected the activity, where the 2,4-dichloro derivative **91m** had twice the activity of doxorubicin, the 4-bromo derivative **91n** had similar activity to that of doxorubicin. Thus, enhanced lipophilicity of the molecules, due to the presence of the halogen atoms, led to substantial improvement in the binding affinity and caused a marked

increase in the anticancer activity of the compounds **91m** and **91n**. Similarly, 3- and 4-methoxybenzylidene derivatives **91c** and **91d** exhibited significant cytotoxic activity ( $IC_{50}$  = 0.63, 0.82  $\mu$ M, respectively) much higher than that of doxorubicin, due to the oxygen atom of the methoxy group that acted as H-bond acceptor with the target protein kinase.<sup>84</sup>



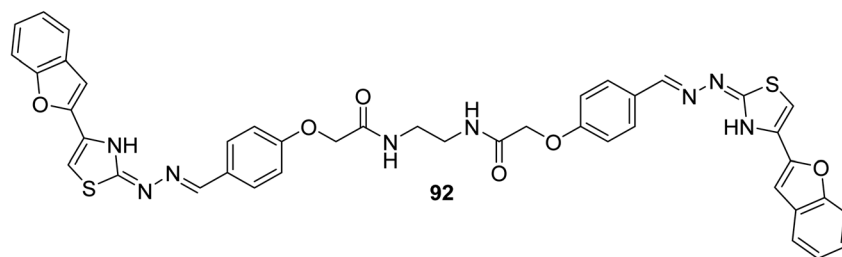
Ar; **91a**=Ph; **91b**=4-MeC<sub>6</sub>H<sub>4</sub>, **91c**=3-MeOC<sub>6</sub>H<sub>4</sub>, **91d**=4-MeOC<sub>6</sub>H<sub>4</sub>, **91e**=2,5-diMeOC<sub>6</sub>H<sub>3</sub>, **91f**=3,4-diMeOC<sub>6</sub>H<sub>3</sub>, **91g**=3,4,5-triMeOC<sub>6</sub>H<sub>2</sub>, **91h**=4-NO<sub>2</sub>C<sub>6</sub>H<sub>4</sub>; **91i**=4-NMe<sub>2</sub>C<sub>6</sub>H<sub>4</sub>, **91j**=4-FC<sub>6</sub>H<sub>4</sub>, **91k**=3-ClC<sub>6</sub>H<sub>4</sub>, **91l**=4-ClC<sub>6</sub>H<sub>4</sub>, **91m**=2,4-diClC<sub>6</sub>H<sub>3</sub>, **91n**=4-BrC<sub>6</sub>H<sub>4</sub>, **91o**= 1-naphyl; **91p**= 2-naphyl; **91q**= 5-Me-2-furyl; **91r**= 2-thienyl; **91s**= 4-pyridyl

(**91m**:  $IC_{50}$  = 0.60  $\mu$ M against Hela)

#### Structure of the 2-(pyrazolyl)benzofuran derivatives **91**

Recently, we reported the synthesis of the bis-amide-based bis-thiazole derivative having benzofuran moiety **92** and was tested for its anticancer activity against colorectal (HCT-116), and breast (MCF-7) cancer cell lines using the MTT assay. The results disclosed that compound **92** had a promising cytotoxicity against HCT-116 cells (with  $IC_{50}$  = 14.26  $\mu$ M) and a moderate activity against MCF-7 (with  $IC_{50}$  = 37.3  $\mu$ M) compared with 5-fluorouracil (5-FU) reference drug (with  $IC_{50}$  values of 11.78  $\mu$ M and 5.81  $\mu$ M against HCT-116 and MCF-7), respectively.<sup>85</sup>



Structure of the *bis*-thiazolyl-benzofuran derivative **92**

### 3. Molecular targeting for benzofurans as anticancer agents

In medicinal chemistry, benzofuran scaffolds are central pharmacophores and favored structures, where they have been useful as active ingredients in several medications with proven clinical efficacy. Recent studies have demonstrated that benzofuran analogues can endure a wide range of pharmacological activities. The remarkable progress of benzofuran derivatives in a variety of disorders in a very short amount of time demonstrates the importance of this area of study to medicinal chemistry. The high demand to explore new and highly efficient anticancer medicines in the human fight against cancers has not diminished. There is a high need for both novel anticancer medications and improved approaches to treating the disease. Recently, the powerful cytotoxic effects of benzofurans against human breast and ovarian cancer cells have been discovered.<sup>86,87</sup> A panel of human tumor cell lines were tested *in vitro* after the researchers developed various new benzofuran derivatives.<sup>88</sup> It was discovered that the presence of a 2-methylimidazole or 2-ethylimidazole ring, as well as the substitution of the imidazolyl-3-position with a naphthylacetyl or methoxyphenacyl group, were necessary for adjusting the level of cytotoxic activity. As benzofuran derivatives have pharmacological activities against cancer, their molecular targets for anticancer activity are summarized in Fig. 3.<sup>89</sup>

#### 3.1. Farnesyltransferase inhibitors

Membrane-bound GTP binding proteins (G-proteins) govern cell development by cycling between an inactive GDP-bound

state and an active GTP-bound state, functioning as molecular switches. Some G-proteins were activated constantly in tumor cells, promoting their cancerous growth.<sup>90,91</sup> A series of benzofuran-based farnesyltransferase inhibitors have been designed and synthesized as antitumor agents. One of these derivatives showed the most potent enzyme inhibitory activity with  $IC_{50}$  of 1.1 nM and antitumor activity in human cancer xenografts in mice.<sup>92</sup>

#### 3.2. Angiogenesis inhibitors

The formation of a new blood supply system, known as angiogenesis, is a hallmark of newly developing tumors. To put it simply, angiogenesis is the driving force behind not only the initial development of a tumor but also its subsequent development, spread, and recurrence.<sup>93</sup> For these reasons, preventing tumor angiogenesis can halt tumor development, growth, and metastasis to other organs.<sup>94</sup> A series of benzofuran derivatives were synthesized and evaluated against cancer proliferation. One of these derivatives, exhibited good inhibitory activity and remarkable selectivity to HUVEC. Hence, it represented a promising structural core to discover a new class of active and selective angiogenesis inhibitors.<sup>95</sup>

#### 3.3. PIM-1 inhibitors

Several carcinogenic processes have been linked to Pim-1, Pim-2, and Pim-3, which are all members of the same family of serine/threonine kinases.<sup>96</sup> The Pim-1 proto-oncogene was first discovered to be a common integration site for slowly converting Maloney murine leukemia virus in murine T cell lymphomas.<sup>97</sup> Human lymphomas and acute leukemias with

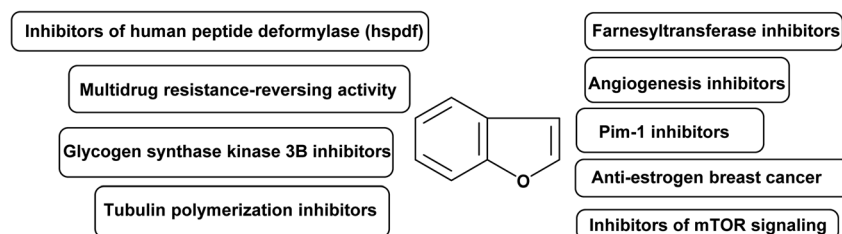


Fig. 3 Summarized molecular targets for benzofurans as anticancer compounds.



Pim-1 overexpression are found throughout a broad spectrum of disease types.<sup>98</sup> A series of benzofuran derivatives were reported to have potent inhibition against Pim-1 and Pim-2 in enzyme assays. Xiang *et al.* 2011 designed new, structurally diverse and more potent benzofuran-based derivatives for the active treatment of prostate cancer and other related diseases caused by deregulation of Pim-1 kinase.<sup>99</sup>

### 3.4. Anti-estrogen breast cancer agents

Breast cancer accounts for 23% of all cancer diagnoses in women and 14% of all cancer deaths, making it the most common cancer in women and the second largest cause of cancer deaths among women (after lung cancer). Treatments for breast cancer often focus on blocking the effects of estrogen by inhibiting aromatase or blocking the ER $\alpha$ . Targeting the ER $\alpha$  subtype, which is overrepresented in breast cancer cells, is crucial. Antagonists for ER $\alpha$  work by blocking the receptor's active site, preventing oestrogen from binding, and blocking the hormone's effect. Estrogen binds to ER at its active site, causing conformational changes that open the complex to attachment of co-activators in breast cancer cells. Therefore, a number of actions were activated, leading to an increase in breast cell proliferation.<sup>100</sup> Leow *et al.* 2013 identified important functional groups present on 5,6-dihydroxybenzofuran, which could be a promising scaffold for designing novel ER ligands chemotherapeutic anticancer.<sup>101</sup>

### 3.5. Tubulin polymerization inhibitors

Eukaryotic cells' microtubule system is crucial for controlling cell structure. Due to their critical role in cell division, microtubules are a crucial part of the mitotic spindle.<sup>102</sup> Since microtubules play a crucial role in mitosis and cell division, they could be a good drug target for treating cancer. As inhibitors of tubulin polymerization, small compounds like benzofurans are appealing. Dihydrobenzofuran ligands constitute a new group of antimetabolic and potential antitumor agents that inhibit tubulin polymerization.<sup>103</sup>

### 3.6. Glycogen synthase kinase 3 $\beta$ inhibitors

Cell cycle regulation, proliferation, death, signaling, and transcription are just some of the many cellular activities that GSK-3 (glycogen synthase kinase) can affect through phosphorylation of a wide number of substrates. In mammals, GSK-3 consists of two distinct isoforms,  $\alpha$  and  $\beta$ .<sup>104</sup> Research in recent years has shown that glycogen synthase kinase 3 (GSK-3) is overexpressed in human colon and pancreatic carcinomas, and that this contributes to cancer cell proliferation and survival. Eldehna *et al.* 2020 described and synthesized benzofuran hybrids as dual CDK2/GSK-3 $\beta$  inhibitors targeting breast cancer.<sup>105</sup>

### 3.7. Multidrug resistance-reversing activity

Both in antimicrobial therapy and in the treatment of cancer, the emergence of resistance to several drugs is a major concern. Several mechanisms of pleiotropic drug resistance in tumour cells have been uncovered in the past decade. P-glycoprotein is

an energy-dependent, membrane-bound efflux pump implicated as a mediator of multidrug resistance (MDR). PGP is an ATP binding cassette 3 member with limited substrate specificity.<sup>106</sup> A series of benzofuryl-ethanolamine analogs of propafenone have been prepared and evaluated for multidrug resistance-reversing activity in two *in vitro* assays.<sup>107</sup>

### 3.8. Inhibitors of human peptide deformylase (HsPDF)

Actinodin, actinodin analogues, or targeted siRNA suppression of expression of human peptide deformylase (HsPDF) has been linked to an antiproliferative effect in cancer cells.<sup>108</sup> HsPDF inhibitors are a promising new class of cancer drugs. Series of benzofuran-4,5-diones derivatives were synthesized as selective inhibitors of human peptide deformylase (HsPDF) as a new class of antitumor agents.<sup>109</sup>

### 3.9. Inhibitors of mTOR signaling

Cell proliferation, metabolism, autophagy, and angiogenesis are all regulated by the mammalian Target of Rapamycin (mTOR).<sup>110</sup> Therefore, mTOR is a significant target in oncology since its signaling is commonly changed in cancer cells. Salomé *et al.* 2014 designed novel benzofuran derivatives as inhibitors of mTOR pathway against a panel of human cancer cells.<sup>111,112</sup>

## 4. Conclusions

The occurrence of benzofuran scaffold in many highly bioactive natural products and synthetic compounds is of a great value for researchers working in the area of drug design, discovery and development. The benzofuran nucleus is a key structural motif for a wide number of approved anticancer drugs that are currently in the market. The mechanistic study proved that some benzofuran derivatives caused significant apoptosis in leukemia HL-60 cell line at 6  $\mu$ M (63.5%) in comparison with control cells (2.6%), without significant side effects. The *in vivo* anticancer activity of several benzofuran derivatives was tested at different doses by the intraperitoneal route, where some benzofurans significantly inhibited lung tumor growth and decreased the average weight and volume without significant side effects. Based on the aforementioned findings; benzofuran derivatives have better anticancer activity than several anticancer reference drugs against panels of more than 40 human cancer cell lines (with IC<sub>50</sub> values in nanomolar scales at low concentrations). Benzofuran scaffolds are highly promising candidates for further development as anticancer agents. Finally, the anticancer efficacies were affected by the electronic nature of the substituents on the benzofuran skeleton where studying the SAR of benzofuran derivatives was reported, in several examples, to enable designing and developing novel, potent and safe anticancer therapeutics. Therefore, much research efforts are still required to be focused on studying the substituents effects that highly enhance the drug-like properties of the benzofuran scaffolds to reach the outmost challenges and prominent benefits to improve human health and reduce suffering.



## Author contributions

Both authors (A. A. A. and K. M. D.) collected the material, wrote, revised and prepared the review for publication.

## Conflicts of interest

There are no conflicts to declare.

## References

- B. Gao, B. Yang, X. Feng and C. Li, *Nat. Prod. Rep.*, 2022, **39**, 139–162.
- L. Cossy and A. Guerinot, *Adv. Heterocycl. Chem.*, 2016, **119**, 107–142.
- K. Chand, A. Hiremathad, M. Singh, M. A. Santos and R. S. Keri, *Pharmacol. Rep.*, 2017, **69**, 281–295.
- Y. H. Miao, Y. H. Hu, J. Yang, T. Liu, J. Sun and X. J. Wang, *RSC Adv.*, 2019, **9**, 27510–27540.
- A. Radadiya and A. Shah, *Eur. J. Med. Chem.*, 2015, **97**, 356–376.
- R. J. Nevagi, S. N. Dighe and S. N. Dighe, *Eur. J. Med. Chem.*, 2015, **97**, 561–581.
- G. S. Hassan, H. H. Georgey and R. F. George, *Bull. Fac. Pharm. Cairo Univ.*, 2018, **56**, 121–127.
- S. Demirayak, L. Yurttas, N. Gundogdu-Karaburun, A. C. Karaburun and I. Kayagil, *J. Enzyme Inhib. Med. Chem.*, 2015, **30**, 816–825.
- X. Zheng, H. Wang, Y. M. Liu, X. Yao, M. Tong, Y. H. Wang and D. F. Liao, *J. Heterocycl. Chem.*, 2015, **52**, 296–301.
- A. Alsayari, A. B. Muhsinah, M. Z. Hassan, M. J. Ahsan, J. A. Alshehri and N. Begum, *Eur. J. Med. Chem.*, 2019, **166**, 417–431.
- L. Ma, L. Tang and Q. Yi, *Front. Pharmacol.*, 2019, **10**, 97.
- T. Qin, A. Rasul, A. Sarfraz, I. Sarfraz, G. Hussain, H. Anwar, A. Riaz, S. Liu, W. Wei, J. Li and X. Li, *Int. J. Biol. Sci.*, 2019, **15**, 2256–2264.
- W. Sha, Y. Zhou, Z. Q. Ling, G. Xie, X. Pang, P. Wang and X. Gu, *Oncotarget*, 2018, **9**, 36331–36343.
- J. J. La Clair, A. L. Rheingold and M. D. Burkart, *J. Nat. Prod.*, 2011, **74**, 2045–2051.
- Y. Li, L. Bao, B. Song, J. Han, H. Li, F. Zhao and H. Liu, *Food Chem.*, 2013, **141**, 1614–1618.
- B. S. Yun, H. C. Kang, H. Koshino, S. H. Yu and I. D. Yoo, *J. Nat. Prod.*, 2001, **64**, 1230–1231.
- Y. Yang, T. Gong, C. Liu and R. Y. Chen, *Chem. Pharm. Bull.*, 2010, **58**, 257–260.
- (a) R. Naik, D. S. Harmalkar, X. Xu, K. Jang and K. Lee, *Eur. J. Med. Chem.*, 2015, **90**, 379–393; (b) X. L. Wang, X. X. Di, T. Shen, S. Q. Wang and X. N. Wang, *Chin. Chem. Lett.*, 2017, **28**, 37–40; (c) Z. Wang, Y. Wang, B. Wang, W. Li, L. Huang and X. Li, *J. Med. Chem.*, 2015, **58**, 8616–8637.
- T. Promchai, P. Janhom, W. Maneerat, R. Rattanajak, S. Kamchonwongpaisan, S. G. Pyne and T. Limtharakul, *Nat. Prod. Res.*, 2020, **34**, 1394–1398.
- E. W. C. Chan, S. K. Wong, J. Tangah, T. Inone and H. T. Chan, *J. Integr. Med.*, 2020, **18**, 189–195.
- C. Benz, Novel pathways in the etiology of cancer, *US Pat.*, US20060024691A1, 2006.
- S. Santagata, M. L. Mendillo, Y. C. Tang, A. Subramanian, C. C. Perley, S. P. Roche, B. Wong, R. Narayan, H. Kwon, M. Koeva and A. Amon, *Science*, 2013, **341**, 1238303.
- W. Li, Z. H. Yang, A. X. Hu and X. W. Yan, *Chem. Biol. Drug Des.*, 2015, **86**, 1339–1350.
- X. L. Xu, Y. R. Yang, X. F. Mo, J. L. Wei, X. J. Zhan and Q. D. You, *Eur. J. Med. Chem.*, 2017, **137**, 45–62.
- K. M. Dawood, *Expert. Opin. Therap. Pat.*, 2013, **23**, 1133–1156.
- K. M. Dawood, *Expert. Opin. Therap. Pat.*, 2019, **29**, 841–870.
- F. M. Thabet, K. M. Dawood, E. M. Ragab, M. S. Nafie and A. A. Abbas, Design and synthesis of new bis(1,2,4-triazolo [3,4-b][1,3,4]thiadiazines) and bis(quinoxalin-2-ylphenoxy) alkanes as anti-breast cancer agents through dual PARP-1 and EGFR target inhibition, *RSC Adv.*, 2022, **12**, 23644–23660.
- H. Behbehani, F. Aryan, K. M. Dawood and H. Ibrahim, *Sci. Rep.*, 2020, **10**, 21691.
- A. A. Abbas and K. M. Dawood, *Expert. Opin. Drug Discov.*, 2022, **17**, 1357–1376.
- Y. Chen, G. Wang, Y. Yuan, G. Zou, W. Yang, Q. Tan, W. Kang and Z. She, *Front. Chem.*, 2022, **10**, 842405.
- T. Q. Lang, G. Y. Luo, W. C. Pu, Z. W. Wang, J. Wang, X. L. Tian, P. Zhang, N. W. Zhao, W. D. Yang and H. F. Chai, *Nat. Prod. Res.*, 2022, **36**, 1205–1214.
- X. Fan, H. He, J. Li, G. Luo, Y. Zheng, J. K. Zhou, J. He, W. Pu and Y. Zhao, *Bioorg. Med. Chem.*, 2019, **27**, 2235–2244.
- T. H. Tseng, C. J. Wang, Y. J. Lee, Y. C. Shao, C. H. Shen, K. C. Lee, S. Y. Tung and H. C. Kuo, *Internat. J. Mol. Sci.*, 2022, **23**, 5102.
- A. Sivaraman, J. S. Kim, D. S. Harmalkar, K. H. Min, J. W. Park, Y. Choi, K. Kim and K. Lee, *J. Nat. Prod.*, 2020, **83**, 3354–3362.
- C. Gao, X. Sun, Z. Wu, H. Yuan, H. Han, H. Huang, Y. Shu, M. Xu, R. Gao, S. Li and J. Zhang, *Front. Pharmacol.*, 2020, **11**, 391.
- H. Cao, R. Ma, S. Chu, J. Xi, L. Yu and R. Guo, *Chin. Chem. Lett.*, 2021, **32**, 2761–2764.
- M. Liu, X. Zhang, S. Chu, Y. Ge, T. Huang, Y. Liu and L. Yu, *Chin. Chem. Lett.*, 2022, **33**, 205–208.
- T. O. Olomola, M. J. Mphahlele and S. Gildenhuys, *Bioorg. Chem.*, 2020, **100**, 103945.
- L. P. Jin, Q. Xie, E. F. Huang, L. Wang, B. Q. Zhang, J. S. Hu, D. C. C. Wan, Z. Jin and C. Hu, *Bioorg. Chem.*, 2020, **95**, 103566.
- Y. Gao, C. Ma, X. Feng, Y. Liu and X. Haimiti, *Chem. Biodivers.*, 2020, **17**, e1900622.
- R. Dharavath, M. Sarasija, M. Ram Reddy, K. Naga Prathima, N. Nagarju, K. Ramakrishna, D. Ashok and S. Daravath, *Med. Chem. Res.*, 2022, **31**, 993–1002.
- S. Mokenapelli, G. Thalari, N. Vadiyaala, J. R. Yerrabelli, V. K. Irlapati, N. Gorityala, S. R. Sagurthi and P. R. Chitneni, *Arch. Pharm.*, 2020, **353**, 2000006.
- M. M. Al-Sanea, G. H. Al-Ansary, Z. M. Elsayed, R. M. Maklad, E. B. Elkadeed, M. A. Abdelgawad,



- S. N. A. Bukhari, M. M. Abdel-Aziz, H. Suliman and W. M. Eldehna, *J. Enzyme Inhib. Med. Chem.*, 2021, **36**, 987–999.
- 44 X. He, Y. Gao, Z. Hui, G. Shen, S. Wang, T. Xie and X. Y. Ye, *Bioorg. Med. Chem. Lett.*, 2020, **30**, 127109.
- 45 B. Y. Kim, N. K. Soung and M. Ahn, PCT WO2021010731A1, 2021.
- 46 W. M. Eldehna, S. T. Al-Rashood, T. Al-Warhi, R. O. Eskandrani, A. Alharbi and A. M. El Kerdawy, *J. Enzyme Inhib. Med. Chem.*, 2021, **36**, 270–285.
- 47 W. M. Eldehna, R. Salem, Z. M. Elsayed, T. Al-Warhi, H. R. Knany, R. R. Ayyad, T. B. Traiki, M. H. Abdulla, R. Ahmad and H. A. Abdel-Aziz, *J. Enzyme Inhib. Med. Chem.*, 2021, **36**, 1423–1434.
- 48 S. Fares, K. B. Selim, F. E. Goda, M. A. El-Sayed, N. A. Alsaif, M. M. Hefnawy, A. A. M. Abdel-Aziz and A. S. El-Azab, *J. Enzyme Inhib. Med. Chem.*, 2021, **36**, 1488–1499.
- 49 F. Wang, K. R. Feng, J. Y. Zhao, J. W. Zhang, X. W. Shi, J. Zhou, D. Gao, G. Q. Lin and P. Tian, *Bioorg. Med. Chem.*, 2020, **28**, 115822.
- 50 Q. Li, X. E. Jian, Z. R. Chen, L. Chen, X. S. Huo, Z. H. Li, W. W. You, J. J. Rao and P. L. Zhao, *Bioorg. Chem.*, 2020, **102**, 104076.
- 51 N. F. El-Sayed, M. El-Hussieny, E. F. Ewies, M. F. El Shehry, H. M. Awad and M. A. Fouad, *Drug Develop. Res.*, 2022, **83**, 485–500.
- 52 O. A. El-Khouly, M. A. Henen, A. A. Magda, M. I. Shabaan and S. M. El-Messery, *Bioorg. Med. Chem.*, 2021, **31**, 115976.
- 53 S. N. A. Bukhari, *RSC Adv.*, 2022, **12**, 10307–10320.
- 54 M. A. Abdelrahman, W. M. Eldehna, A. Nocentini, H. S. Ibrahim, H. Almahli, H. A. Abdel-Aziz, S. M. Abou-Seri and C. T. Supuran, *J. Enzyme Inhib. Med. Chem.*, 2020, **35**, 298–305.
- 55 X. Zhang, H. Huang, Z. Zhang, J. Yan, T. Wu, W. Yin, Y. Sun, X. Wang, Y. Gu, D. Zhao and M. Cheng, *Eur. J. Med. Chem.*, 2021, **220**, 113501.
- 56 H. Gao, X. Zhang, X. J. Pu, X. Zheng, B. Liu, G. X. Rao, C. P. Wan and Z. W. Mao, *Bioorg. Med. Chem. Lett.*, 2019, **29**, 806–810.
- 57 A. Hu, J. He, D. Lin, X. Wei and J. Ye, CN110950825A, 2020.
- 58 A. Carella, V. Roviello, R. Iannitti, R. Palumbo, S. La Manna, D. Marasco, M. Trifuoggi, R. Diana and G. N. Roviello, *Internat. J. Biol. Macromol.*, 2019, **121**, 77–88.
- 59 P. Oliva, R. Romagnoli, S. Manfredini, A. Brancale, S. Ferla, E. Hamel, R. Ronca, F. Maccarinelli, A. Giacomini, F. Rruqa and E. Mariotto, *Eur. J. Med. Chem.*, 2020, **200**, 112448.
- 60 W. M. Eldehna, A. Nocentini, Z. M. Elsayed, T. Al-Warhi, N. Aljaeed, O. J. Alotaibi, M. M. Al-Sanea, H. A. Abdel-Aziz and C. T. Supuran, *ACS Med. Chem. Lett.*, 2020, **11**, 1022–1027.
- 61 M. Shaldam, W. M. Eldehna, A. Nocentini, Z. M. Elsayed, T. M. Ibrahim, R. Salem, R. A. El-Domany, C. Capasso, H. A. Abdel-Aziz and C. T. Supuran, *Eur. J. Med. Chem.*, 2021, **216**, 113283.
- 62 Z. Y. Qi, S. Y. Hao, H. Z. Tian, H. L. Bian, L. Hui and S. W. Chen, *Bioorg. Chem.*, 2020, **94**, 103392.
- 63 B. G. Youssif, A. M. Mohamed, E. E. A. Osman, O. F. Abou-Ghadir, D. H. Elnaggar, M. H. Abdelrahman, L. Treambu and H. A. Gomaa, *Eur. J. Med. Chem.*, 2019, **177**, 1–11.
- 64 Y. Matiichuk, Y. Ostapiuk, T. Chaban, M. Sulyma, N. Sukhodolska and V. Matychuk, *Biointerface Res. Appl. Chem.*, 2020, **10**, 6597–6609.
- 65 U. Farooq, S. Naz, A. Shams, Y. Raza, A. Ahmed, U. Rashid and A. Sadiq, *Biol. Res.*, 2019, **52**, 1–12.
- 66 A. H. Liu, L. H. Liu and C. Y. Liu, *Nat. Prod. Commun.*, 2020, **15**, 1–4.
- 67 G. Zheng, A. Kadir, X. Zheng, P. Jin, J. Liu, M. Maiwulanjiang, G. Yao and H. A. Aisa, *Org. Chem. Front.*, 2020, **7**, 3137–3145.
- 68 A. M. Zaher, R. Sultan, T. Ramadan and A. Amro, *Nat. Prod. Res.*, 2021, **36**, 136–141.
- 69 K. Kumar, J. P. Mishra and R. P. Singh, *Chem. Biol. Interact.*, 2020, **315**, 108898.
- 70 M. Kumari, S. Kamat and C. Jayabaskaran, *Spectrochim. Acta, Part A*, 2022, **274**, 121098.
- 71 A. Garg, S. Garg, N. K. Sahu, S. Rani, U. Gupta and A. K. Yadav, *Internat. J. Pharm.*, 2019, **557**, 238–253.
- 72 S. Wang, J. Zang, M. Huang, L. Guan, K. Xing, J. Zhang, D. Liu and L. Zhao, *Bioorg. Chem.*, 2019, **89**, 102971.
- 73 A. S. Filimonov, A. A. Chepanova, O. A. Luzina, A. L. Zakharenko, O. D. Zakharova, E. S. Ilina, N. S. Dyrkheeva, M. S. Kuprushkin, A. V. Kolotaev, D. S. Khachatryan and J. Patel, *Molecules*, 2019, **24**, 3711.
- 74 A. Pyrczak-Felczykowska, T. A. Reekie, M. Jąkalski, A. Hać, M. Malinowska, A. Pawlik, K. Ryś, B. Guzow-Krzemińska and A. Herman-Antosiewicz, *Internat. J. Mol. Sci.*, 2022, **23**, 1802.
- 75 W. Zhang, J. Chu, A. M. Cyr, H. Yueh, L. E. Brown, T. T. Wang, J. Pelletier and J. A. Porco Jr, *J. Am. Chem. Soc.*, 2019, **141**, 12891–12900.
- 76 G. Schulz, C. Victoria, A. Kirschning and E. Steinmann, *Nat. Prod. Rep.*, 2021, **38**, 18–23.
- 77 X. Yan, C. Yao, C. Fang, M. Han, C. Gong, D. Hu, W. Shen, L. Wang, S. Li and S. Zhu, *Internat. J. Biol. Sci.*, 2022, **18**, 585.
- 78 C. Pandit and K. M. Kapadiya, *Folia Med.*, 2019, **61**, 551–558.
- 79 S. K. Siddiqui, V. J. SahayaSheela, S. Kolluru, G. N. Pandian, T. R. Santhoshkumar, V. M. Dan and C. V. Ramana, *Bioorg. Med. Chem. Lett.*, 2020, **30**, 127431.
- 80 Y. Y. Shao, Y. Yin, B. P. Lian, J. F. Leng, Y. Z. Xia and L. Y. Kong, *Eur. J. Med. Chem.*, 2020, **190**, 112105.
- 81 O. M. Abdelhafez, E. Y. Ahmed, N. A. A. Latif, R. K. Arafa, Z. Y. Abd Elmageed and H. I. Ali, *Bioorg. Med. Chem.*, 2019, **27**, 1308–1319.
- 82 S. Kuduk and X. Zhang, PCT WO2021240429A1, 2021.
- 83 E. Y. Ahmed, O. M. Abdelhafez, D. Zaafar, A. M. Serry, Y. H. Ahmed, R. F. A. El-Telbany, Z. Y. Abd Elmageed and H. I. Ali, *Arch. Pharm.*, 2022, **355**, 2100327.
- 84 H. A. S. Abbas and S. S. Abd El-Karim, *Bioorg. Chem.*, 2019, **89**, 103035.
- 85 K. M. Dawood, M. A. Raslan, A. A. Abbas, B. E. Mohamed and M. S. Nafie, *Anticancer Agents Med. Chem.*, 2023, **23**, 328–345.





- 86 G. N. Zhang, L. Y. Zhong, S. A. Bligh, Y. L. Guo, C. F. Zhang, M. Zhang, Z. T. Wang and L. S. Xu, *Phytochem*, 2005, **66**, 1113–1120.
- 87 S. Van Miert, S. Van Dyck, T. J. Schmidt, R. Brun, A. Vlietinck, G. Lemièrre and L. Pieters, *Bioorg. Med. Chem.*, 2005, **13**, 661–669.
- 88 W. C. Wan, W. Chen, L. X. Liu, Y. Li, L. J. Yang, X. Y. Deng, H. B. Zhang and X. D. Yang, *Med. Chem. Res.*, 2014, **23**, 1599–1611.
- 89 H. Khanam, *Eur. J. Med. Chem.*, 2015, **97**, 483–504.
- 90 R. Bar-Shavit, M. Maoz, A. Kancharla, J. K. Nag, D. Agranovich, S. Grisaru-Granovsky and B. Uziely, *Int. J. Mol. Sci.*, 2016, **17**, 1320.
- 91 M. S. Nafie, M. A. Tantawy and G. A. Elmgeed, *Steroids*, 2019, **152**, 108485.
- 92 K. Asoh, M. Kohchi, I. Hyoudoh, T. Ohtsuka, M. Masubuchi, K. Kawasaki, H. Ebike, Y. Shiratori, T. A. Fukami, O. Kondoh, T. Tsukaguchi, N. Ishii, Y. Aoki, N. Shimma and M. Sakaitani, *Bioorg. Med. Chem. Lett.*, 2009, **19**, 1753–1757.
- 93 P. Carmeliet and R. K. Jain, *Nature*, 2000, **407**, 249–257.
- 94 D. T. Debela, S. G. Muzazu, K. D. Heraro, M. T. Ndalama, B. W. Mesele, D. C. Haile, S. K. Kitui and T. Manyazewal, *SAGE Open Med.*, 2021, **9**, 20503121211034366.
- 95 Y. Chen, S. Chen, X. Lu, H. Cheng, Y. Ou, H. Cheng and G.-C. Zhou, *Bioorg. Med. Chem. Lett.*, 2009, **19**, 1851–1854.
- 96 N. S. Magnuson, Z. Wang, G. Ding and R. Reeves, *Future Oncol.*, 2010, **6**, 1461–1478.
- 97 H. T. Cuyppers, G. Selten, W. Quint, M. Zijlstra, E. R. Maandag, W. Boelens, P. van Wezenbeek, C. Melief and A. Berns, *Cell*, 1984, **37**, 141–150.
- 98 R. Amson, F. Sigaux, S. Przedborski, G. Flandrin, D. Givol and A. Telerman, *Proceed. Nat. Acad. Sci.*, 1989, **86**, 8857–8861.
- 99 Y. Xiang, B. Hirth, G. Asmussen, H. P. Biemann, K. A. Bishop, A. Good, M. Fitzgerald, T. Gladysheva, A. Jain, K. Jancsics, J. Liu, M. Metz, A. Papoulis, R. Skerlj, J. D. Stepp and R. R. Wei, *Bioorg. Med. Chem. Lett.*, 2011, **21**, 3050–3056.
- 100 J. Russo and I. H. Russo, *J. Steroid Biochem. Mol. Biol.*, 2006, **102**, 89–96.
- 101 M. L. Leow, H. L. C. Chin, P. S. Yu, K. K. Pasunooti, R. X. Z. Tay, D. Zhang, H. S. Yoon and X. W. Liu, *Curr. Med. Chem.*, 2013, **20**, 2820–2837.
- 102 S. Honore, E. Pasquier and D. Braguer, *Cell. Mol. Life Sci.*, 2005, **62**, 3039–3056.
- 103 L. Pieters, S. Van Dyck, M. Gao, R. Bai, E. Hamel, A. Vlietinck and G. Lemièrre, *J. Med. Chem.*, 1999, **42**, 5475–5481.
- 104 J. R. Woodgett, *EMBO J.*, 1990, **9**, 2431–2438.
- 105 W. M. Eldehna, S. T. Al-Rashood, T. Al-Warhi, R. O. Eskandrani, A. Alharbi and A. M. El Kerdawy, *J. Enzyme. Inhib. Med. Chem.*, 2021, **36**, 271–286.
- 106 R. L. Juliano and V. Ling, *Biochim. Biophys. Acta, Biomembr.*, 1976, **455**, 152–162.
- 107 G. Ecker, P. Chiba, M. Hitzler, D. Schmid, K. Visser, H. P. Cordes, J. Csöllei, J. K. Seydel and K. J. Schaper, *J. Med. Chem.*, 1996, **39**, 4767–4774.
- 108 M. D. Lee, Y. She, M. J. Soskis, C. P. Borella, J. R. Gardner, P. A. Hayes, B. M. Dy, M. L. Heaney, M. R. Philips, W. G. Bornmann and F. M. Sirotnak, *J. Clin. Invest.*, 2004, **114**, 1107–1116.
- 109 C. Antczak, D. Shum, B. Bassit, M. G. Frattini, Y. Li, E. de Stanchina, D. A. Scheinberg and H. Djaballah, *Bioorg. Med. Chem. Lett.*, 2011, **21**, 4528–4532.
- 110 M. E. Welker and G. Kulik, *Bioorg. Med. Chem.*, 2013, **21**, 4063–4091.
- 111 C. Salomé, V. Narbonne, N. Ribeiro, F. Thuaud, M. Serova, A. de Gramont, S. Faivre, E. Raymond and L. Désaubry, *Eur. J. Med. Chem.*, 2014, **74**, 41–49.
- 112 C. Salomé, N. Ribeiro, T. Chavagnan, F. Thuaud, M. Serova, A. de Gramont, S. Faivre, E. Raymond and L. Désaubry, *Eur. J. Med. Chem.*, 2014, **81**, 181–191.

